Atmospheric
Chemistry
and Physics
Discussions

Open Access

EGU

1 **Biogenic halocarbons from the Peruvian upwelling region**

2 **as tropospheric halogen source**

3

4 **Helmke Hepach[1], Birgit Quack[1], Susann Tegtmeier[1], Anja Engel[1], Astrid**

5 **Bracher[2], Steffen Fuhlbrügge[1], Luisa Galgani[1], Elliot Atlas[3], Johannes**

6 **Lampel[4,5], Udo Frieß[4], and Kirstin Krüger[6]**

7 Correspondence to: H. Hepach (hhepach@geomar.de)

8

9 [1] GEOMAR Helmholtz Centre for Ocean Research Kiel, Germany

10 [2] Alfred Wegener Institute (AWI), Helmholtz Centre for Polar and Marine Research

11 Bremerhaven, Germany and Institute of Environmental Physics, University of Bremen,

12 Germany

13 [3] Rosenstiel School of Marine and Atmospheric Science (RSMAS), University of Miami,

14 USA

15 [4] Institute of Environmental Physics, University of Heidelberg, Germany

16 [5] now at Max Planck Institute for Chemistry, Mainz, Germany

17 [6] Department of Geosciences, University of Oslo, Oslo, Norway

18

19

20

21

22

23

24

25

26

27

Atmospheric
Chemistry
and Physics
Discussions

1 **Abstract**

2 Halocarbons, halogenated short-chained hydrocarbons, are produced naturally in the oceans

3 by biological and chemical processes. They are emitted from surface seawater into the

4 atmosphere, where they take part in numerous chemical processes such as ozone destruction

5 and the oxidation of mercury and dimethyl sulfide. Here we present oceanic and atmospheric

6 halocarbon data for the Peruvian upwelling obtained during the M91 cruise onboard the

7 research vessel *Meteor* in December 2012. Surface waters during the cruise were

8 characterized by moderate concentrations of bromoform ($CHBr_3$) and dibromomethane

9 (CH_2Br_2) correlating with diatom biomass derived from marker pigment concentrations,

10 which suggests this phytoplankton group as likely source. Concentrations measured for the

11 iodinated compounds methyl iodide (CH_3I) of up to 35.4 pmol L^{-1}, chloroiodomethane

12 (CH_2ClI) of up to 58.1 pmol L^{-1} and diiodomethane (CH_2I_2) of up to 32.4 pmol L^{-1} in water

13 samples were much higher than previously reported for the tropical Atlantic upwelling

14 systems. Iodocarbons also correlated with the diatom biomass and even more significantly

15 with dissolved organic matter (DOM) components measured in the surface water. Our results

16 suggest a biological source of these compounds as significant driving factor for the observed

17 large iodocarbon concentrations. Elevated atmospheric mixing ratios of CH_3I (up to 3.2 ppt),

18 CH_2ClI (up to 2.5 ppt) and CH_2I_2 (3.3 ppt) above the upwelling were correlated with seawater

19 concentrations and high sea-to-air fluxes. The enhanced iodocarbon production in the

20 Peruvian upwelling contributed significantly to tropospheric iodine levels.

21

22 **1 Introduction**

23 Brominated and iodinated short-lived organic compounds (halocarbons) from the oceans

24 contribute to tropospheric and stratospheric chemistry (von Glasow et al., 2004; Saiz-Lopez et

25 al., 2012b; Carpenter and Reimann, 2014). They are significant carriers of iodine and bromine

26 into the marine atmospheric boundary layer (Salawitch, 2006; Jones et al., 2010; Yokouchi et

27 al., 2011; Saiz-Lopez et al., 2012b), where they and their degradation products may also be

28 involved in aerosol and ultra-fine particle formation (O'Dowd et al., 2002; Burkholder et al.,

29 2004). Furthermore, the short-lived organic compounds are a source for bromine and iodine in

30 the free troposphere, and thus play an important role for ozone chemistry and other processes

31 such as the oxidation of several atmospheric constituents (Saiz-Lopez et al., 2012a).

32 Numerous modelling studies over the last years have shown that brominated short-lived

33 compounds and their degradation products can be entrained into the stratosphere and enhance

Atmospheric
Chemistry
and Physics
Discussions

Open Access

EGU

1   the halogen-driven ozone destruction (Carpenter and Reimann, 2014; Hossaini et al., 2015).

2   Recently, it was suggested that also oceanic iodine in organic or inorganic form can contribute

3   to the stratospheric halogen loading, however only in small amounts due to its strong

4   degradation (Tegtmeier et al., 2013; Saiz-Lopez et al., 2015).

5   While different source and sink processes determine the distribution of halocarbons in the

6   oceanic surface water, the underlying mechanisms are largely unresolved. Biological activity

7   plays a role for the production of bromoform ($CH Br_3$), dibromomethane (CH_2Br_2), methyl

8   iodide (CH_3I), chloroiodomethane (CH_2ClI) and diiodomethane (CH_2I_2) (Gschwend et al.,

9   1985; Tokarczyk and Moore, 1994; Moore et al., 1996), while CH_3I also originates from

10   photochemical reactions with dissolved organic matter (DOM) (Moore and Zafiriou, 1994;

11   Bell et al., 2002; Shi et al., 2014).

12   Biologically mediated halogenation of DOM (Lin and Manley, 2012; Liu et al., 2015) and

13   bromination of compounds such as β-diketones via enzymes such as bromoperoxidase (BPO)

14   within or outside the algal cells (Theiler et al., 1978) are among the potentially important

15   production processes of $CHBr_3$ and CH_2Br_2. Air-sea gas exchange into the atmosphere is the

16   most important sink for both compounds (Quack and Wallace, 2003; Hepach et al., 2015).

17   The biological formation of CH_3I has been investigated during laboratory and field studies

18   (Scarratt and Moore, 1998; Amachi et al., 2001; Fuse et al., 2003; Smythe-Wright et al., 2006;

19   Brownell et al., 2010; Hughes et al., 2011) identifying phyto- and bacterioplankton as

20   producers, revealing large variability in biological production rates. However, biogeochemical

21   modelling studies suggest that photochemistry may be more important for global CH_3I

22   production (Stemmler et al., 2014). Due to their much shorter lifetime in surface water and the

23   atmosphere, fewer studies investigated production processes of CH_2I_2 and CH_2ClI. CH_2I_2 has

24   been suggested to be produced both by phytoplankton (Moore et al., 1996) and bacteria (Fuse

25   et al., 2003; Amachi, 2008). The main source for CH_2ClI is likely its production during the

26   photolysis of CH_2I_2 with a yield of 35 % based on a laboratory study (Jones and Carpenter,

27   2005). CH_2ClI has also been detected in phytoplankton cultures (Tokarczyk and Moore, 1994)

28   where it may originate from direct production or also from CH_2I_2 conversion. The main sink

29   for both CH_2I_2 and CH_2ClI is their photolytic destruction in the surface ocean resulting in

30   lifetimes of less than 10 min (CH_2I_2) and 9 h (CH_2ClI), respectively, in the tropical ocean

31   (Jones and Carpenter, 2005; Martino et al., 2006). Other sinks for these three iodocarbons are

32   air-sea gas exchange and chloride substitution. The latter may play an important role for CH_3I

33   in low latitudes at low wind speeds (Zafiriou, 1975; Jones and Carpenter, 2007).

1   Oceanic measurements of natural halocarbons are sparse (Ziska et al., 2013), but reveal that

2   especially tropical and subtropical upwelling systems are potentially important source regions

3   (Quack et al., 2007a; Raimund et al., 2011). Previously observed high tropospheric iodine

4   monoxide (IO) levels in the tropical East Pacific have been related to short-lived iodinated

5   compounds in surface waters (Schönhardt et al., 2008; Dix et al., 2013). However, iodocarbon

6   fluxes have not been considered high enough to explain observed IO concentrations (Jones et

7   al., 2010; Mahajan et al., 2010; Grossmann et al., 2013; Lawler et al., 2014), and recent global

8   modelling studies suggested abiotic sources contributing on average about 75 % to the IO

9   budget (Prados-Roman et al., 2015). Such abiotic sources could be emissions of hypoiodous

10   acid (HOI) and molecular iodine (I_2) as recently confirmed by a laboratory study (Carpenter et

11   al., 2013).

12   This paper characterizes the Peruvian upwelling region between 5.0° S, 82.0° W and 16.2° S,

13   76.8° W with regard to the two brominated compounds $CHBr_3$ and CH_2Br_2 and the iodinated

14   compounds CH_3I, CH_2ClI and CH_2I_2 in water and atmosphere. The latter two compounds

15   were measured for the first time in this region. Possible oceanic sources based on the analysis

16   of phytoplankton species composition and different DOM components were evaluated and

17   identified. Sea-to-air fluxes of these halogenated compounds were derived and their

18   contribution to the tropospheric iodine loading above the tropical East Pacific by combining

19   halocarbon and IO measurements and model calculations were estimated.

20

21   **2   Methods**

22   The M91 cruise of the RV *Meteor* from December 1 to 26, 2012 investigated the surface

23   ocean and atmosphere of the Peruvian upwelling region (Bange, 2013). From the

24   northernmost location of the cruise at 5.0° S and 82.0° W, the ship moved to the southernmost

25   position at 16.2° S and 76.8° W with several transects perpendicular to the coast, alternating

26   between open ocean and coastal upwelling (Fig. 1). All underway measurements were taken

27   from a continuously operating pump in the ship's hydrographic shaft from a depth of 6.8 m.

28   Sea surface temperature (SST) and sea surface salinity (SSS) were measured continuously

29   with a SeaCAT thermosalinograph from Seabird Electronics (SBE).

30   Deep samples were taken from 4 to 10 depths between 1 and 2000 m from 12 L Niskin bottles

31   attached to a 24-bottle-rosette sampler equipped with a CTD and an oxygen sensor from SBE.

32   Halocarbon samples were collected at 24 of the total 98 casts. The uppermost sample from the

33   depth profiles (between 1 and 10 m) was included in the surface water measurements.

Atmospheric
Chemistry
and Physics
Discussions

2.1 Analysis of halocarbon samples

Halocarbon samples were taken three hourly from sea surface water and air. Surface water samples were analyzed on board with a purge and trap system attached to a GC-MS (combined gas chromatography and mass spectrometry) described in more detail in Hepach et al. (2014). The depth profile samples were analyzed with a similar setup: a purge and trap system was attached to a GC equipped with an ECD (electron capture detector). The precision of the measurements lay within 10 % for all five halocarbons determined from duplicates and both systems were calibrated using the same liquid standards in methanol. Halocarbon measurements in seawater started only on December 9 due to set up problems. Atmospheric halocarbon samples were taken on the monkey deck at a height of 20 m using a metal bellows pump from December 1, and were analyzed at the Rosenstiel School of Marine and Atmospheric Science (RSMAS) as described in Schauffler et al. (1998). For further details of atmospheric measurements see Fuhlbrügge et al. (2015a). Quantification was achieved using the NOAA standard SX3573 from GEOMAR.

2.2 Biological parameters

Phytoplankton composition was derived from pigment concentrations. Samples were taken in parallel with the halocarbon samples in the sea surface and up to six samples in depths between 3 and 200 m. Water was filtered with GF/F filters, which were stored at -80 °C until analysis after shock-freezing in liquid nitrogen. Pigments as described in Taylor et al. (2011) were analyzed using a HPLC technique according to Barlow et al. (1997). We used the diagnostic pigment analysis by Vidussi et al. (2001), subsequently refined by Uitz et al. (2006) by introducing pigment specific weight coefficients, to determine the chlorophyll *a* (Chl *a*) concentration of seven groups of phytoplankton which are assumed to build up the entire phytoplankton community in ocean waters. Identified phytoplankton groups include diatoms, chlorophytes, dinoflagellates, haptophytes, cyanobacteria, cryptophytes and chrysophytes. Total chlorophyll a (TChl *a*) concentrations were calculated from the sum of the pigment concentrations of monovinyl Chl *a*, divinyl Chl *a* and chlorophyllide *a*.

Samples for the identification of DOM components were taken at 37 stations from a rubber boat from subsurface water at approximately 20 cm (further called "subsurface"). All samples were processed onboard and analyzed back in the home laboratory. Samples were analyzed for dissolved and total organic carbon (DOC and TOC), total dissolved nitrogen (TDN), total nitrogen (TN), total, dissolved and particulate high molecular weight (HMW, >1kDa)

Atmospheric
Chemistry
and Physics
Discussions

1   combined carbohydrates (TCCHO, DCCHO and PCCHO) applying a high-temperature

2   catalytic oxidation method using a TOC analyzer (TOC-V$_{CSH}$) from Shimadzu, as well as

3   total, dissolved and particulate combined HMW uronic acids (TURA, DURA and PURA), i.e.

4   galacturonic acid and glucuronic acid. These were analyzed by High Performance Anion

5   Exchange Chromatography coupled with Pulsed Amperometric Detection (HPAEC-PAD)

6   after Engel and Händel (2011). For a more detailed description of both the sampling method

7   and analysis see Engel and Galgani (2015).

8   **2.3   Correlation analysis**

9   Correlation analyses between all halocarbons, biological proxies and ambient parameters were

10   carried out using Matlab® for all collocated surface and depth samples. All datasets were

11   tested for normal distribution using the Lilliefors-test. Since most of the data were not

12   distributed normally, Spearman's rank correlation (hereinafter called r$_s$) was used. All

13   correlations with a significance level of smaller than 5 % ($p < 0.05$) were regarded as

14   significant.

15   **2.4   Calculation of sea-to-air fluxes**

16   Sea-to-air fluxes F of halocarbons were calculated according to equation 1 with k_w as the gas

17   exchange coefficient parameterized according to Nightingale et al. (2000), c_w the water

18   concentrations from the halocarbon underway measurements, c_{atm} from the simultaneous

19   atmospheric measurements and H as the Henry's law constant to derive the equilibrium

20   concentration.

21
$$F = k_w \cdot (c_w - \frac{c_{atm}}{H}) \qquad\qquad (1)$$

22   The gas exchange coefficient usually applied to derive carbon dioxide fluxes was adjusted for

23   halocarbons using Schmidt number corrections as calculated in Quack and Wallace (2003),

24   and Henry's law coefficients as reported for each of the compounds by Moore et al. (1995)

25   were applied. Wind speed and air pressure were averaged to 10 min intervals for the

26   calculation of the instantaneous fluxes.

27   **2.5   FLEXPART simulations of tropospheric iodine**

28   The atmospheric transport of the iodocarbons from the oceanic surface into the Marine

29   Atmospheric Boundary Layer (MABL) was simulated with the Lagrangian particle dispersion

Atmospheric
Chemistry
and Physics
Discussions

1 model FLEXPART (Stohl et al., 2005) which has been used extensively in studies of long-

2 range and mesoscale transport (Stohl and Trickl, 1999). FLEXPART is an off-line model

3 driven by external meteorological fields. It includes parameterizations for moist convection,

4 turbulence in the boundary layer, dry deposition, scavenging, and the simulation of chemical

5 decay. We simulate trajectories of a multitude of air parcels describing transport and chemical

6 decay of the emitted oceanic iodocarbons. For each data point of the observed sea-to-air flux,

7 100000 air parcels were released over the duration of the M91 cruise from a 0.1° x 0.1° grid

8 box at the ocean surface centered at the measurement location. We used FLEXPART version

9 9.2 and the runs are driven by the ECMWF reanalysis product ERA-Interim (Dee et al., 2011)

10 given at a horizontal resolution of 1° x 1° on 60 model levels. Transport, dispersion and

11 convection of the air parcels are calculated from the 6-hourly fields of horizontal and vertical

12 wind, temperature, specific humidity, convective and large scale precipitation and others. The

13 chemical decay of the iodocarbons was prescribed by their atmospheric lifetime which was set

14 to 4 days, 9 hours and 10 min for CH_3I, CH_2ClI, and CH_2I_2, respectively, according to current

15 estimates (Jones and Carpenter, 2005; Martino et al., 2006; Carpenter and Reimann, 2014).

16 After degradation of the iodocarbons, the released iodine was simulated as inorganic iodine

17 (I_y) tracer with a prescribed lifetime in the marine boundary layer of two days (personal

18 communication R. von Glasow). Thus we did not include detailed tropospheric iodine

19 chemistry, explicit removal of HOI, HI, $IONO_2$, and I_xO_y through scavenging or

20 heterogeneous recycling of HOI, $IONO_2$, and INO_2 on aerosols (Saiz-Lopez et al., 2014). In

21 order to estimate the uncertainties arising from this simplification, we conducted two

22 additional simulations, one with a very short lifetime of one day and one with a longer

23 lifetime of three days. Following model simulations of halogen chemistry for air masses from

24 different oceanic regions in Sommariva and von Glasow (2012), IO corresponds to 20 % of

25 the I_y budget in the marine boundary layer on a daytime average. The IO to I_y ratio shows

26 moderate changes with daytime resulting in highest IO proportion at sunrise (~ 30 %) and

27 lowest IO proportion around noon (~ 15 %) (see Fig. S6 in Sommariva and von Glasow

28 (2012)). The ratio shows only very small variations for different air mass origins and thus the

29 chemical conditions such as ozone and nitrogen species concentrations. Additionally, the ratio

30 does not change much with altitude within the marine boundary layer. Based on the above

31 estimates from Sommariva and von Glasow (2012), we used the IO to I_y ratio as a function of

32 daytime to estimate IO from I_y every 3 hours. Daily averages of the IO abundance were

33 compared to the MAX-DOAS IO measurements on board described in the next section.

Atmospheric
Chemistry
and Physics
Discussions

Open Access

EGU

2.6 MAX-DOAS Measurements of IO

Multi-AXis Diffential Optical Absorption Spectroscopy (MAX-DOAS) (Hönninger, 2002; Platt and Stutz, 2008) observations were conducted continuously at daytime from November 30 to December 25 2012 in order to quantify tropospheric abundances of IO, BrO, HCHO, Glyoxal, NO_2 and HONO along the cruise track, and for aerosol profiles also of O_4. The MAX-DOAS instrument and the measurement procedure are described in Grossmann et al. (2013) and Lampel et al. (2015).

The primary quantity derived from MAX-DOAS measurements is the differential slant column density (dSCD), which represents the difference in path-integrated concentrations between two measurements in off-axis and zenith direction. From the MAX-DOAS observations of O_4 dSCD aerosol extinction profiles to estimate the quality of visibility were inferred using an optimal estimation approach described in Frieß et al. (2006) and Yilmaz (2012) after applying a correction factor of 1.25 to the O_4 dSCDs (Clémer et al., 2010). IO was analyzed in the spectral range from 418 – 438 nm following the settings in Lampel et al. (2015). IO was found up to 6 times above the detection limit (twice the measurement error).

3 The tropical East Pacific – general description and state during M91

The tropical East Pacific is characterized by one of the strongest and most productive all-year-prevailing eastern boundary upwelling systems of the world (Bakun and Weeks, 2008). Temperatures drop to less than 16 °C when cold water from the Humboldt current is transported to the surface due to Ekman transport caused by strong equatorward winds (Tomczak and Godfrey, 2005), which is also connected with an upward transport of nutrients (Chavez et al., 2008). As a consequence of the enhanced nutrient supply and the high solar insolation, phytoplankton blooms, indicated by high Chl *a* values, can be observed at the surface especially in the boreal winter months (Echevin et al., 2008). A strong oxygen minimum zone (OMZ) is formed due to enhanced primary production, sinking particles and weak circulation (Karstensen et al., 2008).

Low SSTs of mean (min – max) 19.4 (15.0 – 22.4) °C and high TChl *a* values of on average 1.80 (0.06 – 12.65) µg L^{-1} (Table 1, Fig. 1) were measured during our cruise. Diatoms were dominating the TChl *a* concentration in the surface water with a mean of 1.66 (0.00 – 10.47) µg Chl *a* L^{-1}, followed by haptophytes (mean: 0.25 µg Chl *a* L^{-1}), chlorophytes (mean: 0.19 µg Chl *a* L^{-1}), cyanobacteria (mean: 0.09 µg Chl *a* L^{-1}), dinoflagellates (mean: 0.08 µg Chl *a* L^{-1}), cryptophytes (mean: 0.03 µg Chl *a* L^{-1}), and finally chrysophytes (mean: 0.03 µg Chl *a*

Atmospheric
Chemistry
and Physics
Discussions

1   L^{-1}). Diatoms were observed at all stations with concentrations above 0.5 μg Chl a L^{-1} to

2   contribute more than 50 % of the algal biomass. They correlated very well with TChl a (Table

3   2) and with cryptophytes, which were elevated in very similar regions. Abundance of these

4   phytoplankton groups was strongly anticorrelated with SST and SSS, indicating a close

5   conjunction with the colder and more saline upwelling waters. Nutrients (nitrate, nitrite,

6   ammonium and phosphate) were also measured during the cruise (see Czeschel et al. (2015)

7   for further information). A weak anticorrelation of phytoplankton group with the ratio of

8   dissolved inorganic nitrogen and phosphate (sum of nitrate, nitrite and ammonium divided by

9   phosphate, DIN:DIP) (Table 2) indicated that diatoms and cryptophytes were more abundant

10   in aged upwelling, where nutrients were already slightly depleted or used up. The TChl a

11   maximum was generally found in the surface ocean except for four stations with overall low

12   TChl a (< 0.5 μg L^{-1}) where a subsurface maximum around 30 and 50 m was identified.

13   All regions with SSTs below the mean of 19.4 °C are considered as upwelling in the

14   following sections for identifying different significant regions for halocarbon production.

15   Based on this criterion, four upwelling regions (I – IV) close to the coast were classified (Fig.

16   1). The most intense upwelling (lowest SSTs, high nutrient concentrations) appeared in the

17   northernmost region of the cruise track, region I, while higher TChl a and lower nutrients

18   indicate a fully developed bloom in the southern part of the cruise (upwelling regions III and

19   IV). Upwelling region II was characterized by a lower DIN:DIP ratio in contrast to region I.

20   SSS with a mean of 34.95 (34.10 and 35.50) is lowest in upwelling region IV, which is likely

21   influenced by local river input such as the rivers Pisco, Cañete and Matagente, and may

22   explain the observed low salinities due to enhanced fresh water input in boreal winter

23   (Bruland et al., 2005).

24

25   **4   Halocarbons in the surface water and depth profiles during M91**

26   **4.1   Halocarbon distribution in surface water**

27   Measurements of halocarbons in the tropical East Pacific are very sparse and no data were

28   available for the Peruvian upwelling system before our campaign. Sea surface concentrations

29   of $CHBr_3$ with a mean of 6.6 (0.2 – 21.5) and of CH_2Br_2 of 4.3 (0.2 – 12.7) pmol L^{-1} were

30   measured during M91 (Table 1, Fig. 2). These values are low in comparison to 44.7 pmol L^{-1}

31   $CHBr_3$ in tropical upwelling systems in the Atlantic, while our measurements of CH_2Br_2

32   compare better to these upwelling systems, from which maximum concentrations of 9.4 pmol

1   L^{-1} were reported (Quack et al., 2007a; Carpenter et al., 2009; Hepach et al., 2014, 2015).

2   $CHBr_3$ (0.2– 20.7 pmol L^{-1}) and CH_2Br_2 (0.7 – 6.5 pmol L^{-1}) concentrations in the tropical

3   East Pacific open ocean and Chilean coastal waters during a cruise from Punta Arenas, Chile

4   to Seattle, USA in April 2010 (Liu et al., 2013) compare well to our data. Some

5   measurements also exist for the tropical West Pacific with on average 0.5 to 3 times the

6   $CHBr_3$ and 0.2 to 1 times the CH_2Br_2 during our cruise with the high average originating from

7   a campaign close to the coast with macroalgal and anthropogenic sources (Krüger and Quack,

8   2013; Fuhlbrügge et al., 2015b). $CHBr_3$ and CH_2Br_2 have been proposed to have similar

9   sources (Moore et al., 1996; Quack et al., 2007b). However, during our cruise, the correlation

10 between the two compounds was comparatively weak ($r_s = 0.56$), consistent with the findings

11 of Liu et al. (2013), who ascribed the weaker correlation of these two compounds to formation

12 in a common ecosystem rather than to the exact same biological sources. Maxima of CH_2Br_2

13 were observed in both upwelling regions III and IV, while $CHBr_3$ was highest in the most

14 southerly upwelling IV (Fig. 2).

15 While we found the Peruvian upwelling and the adjacent waters to be only a moderate source

16 region for bromocarbons, iodocarbons were observed in high concentration of 10.9 (0.4 –

17 58.1) for CH_2ClI, 9.8 (1.1 – 35.4) for CH_3I and 7.7 (0.2 – 32.4) pmol L^{-1} for CH_2I_2 (Table 1,

18 Fig. 3a). These concentrations identify the Peruvian upwelling as a significant source region

19 of iodocarbons, especially considering the very short lifetimes of CH_2I_2 (10 min) and CH_2ClI

20 (9 h) in tropical surface water (Jones and Carpenter, 2005). Hot spots were upwelling regions

21 III and even more the less fresh upwelling of region IV (Fig. 2 and 3).

22 The occurrence of CH_3I in the tropical oceans (up to 36.5 pmol L^{-1}) has previously been

23 attributed to a predominantly photochemical source (Richter and Wallace, 2004; Jones et al.,

24 2010), explaining its global hot spots in the subtropical gyres and close to the tropical western

25 boundaries of the continents (Ziska et al., 2013; Stemmler et al., 2014). Previous

26 measurements in the East Pacific obtained concentrations of up to 21.7 and of up to 8.8 pmol

27 L^{-1} (Butler et al., 2007), but not directly in the upwelling.

28 No oceanic observations of CH_2ClI and CH_2I_2 have been published so far for the tropical East

29 Pacific. Concentrations of CH_2ClI of up to 24.5 pmol L^{-1} were measured in the tropical and

30 subtropical Atlantic ocean (Abrahamsson et al., 2004; Chuck et al., 2005; Jones et al., 2010)

31 and up to 17.1 pmol L^{-1} for CH_2I_2 (Jones et al., 2010; Hepach et al., 2015), which is lower but

32 in the range of our measurements from the Peruvian upwelling.

1   Correlations between the compounds indicate similar sources for all measured halocarbons,

2   except for CH_2Br_2, with upwelling region IV as hot spot area (Fig. 2). The strongest

3   correlation was found for CH_3I with CH_2ClI ($r_s = 0.83$). CH_2I_2 and CH_2ClI are often found to

4   correlate very well with each other (Tokarczyk and Moore, 1994; Moore et al., 1996; Archer

5   et al., 2007), mostly attributed to the formation of CH_2ClI during photolysis of CH_2I_2. In

6   comparison, the weaker correlation between CH_2ClI and CH_2I_2 ($r_s = 0.59$) during our cruise

7   may be the result of additional sources for CH_2ClI (see also section 5).

8   **4.2   Halocarbon distribution in depth profiles**

9   Depth profiles of halocarbons reveal maxima at the surface and around the Chl *a* maximum,

10   usually attributed to biological production of these compounds. $CHBr_3$ and CH_2Br_2 profiles

11   (not shown) showed distinct maxima in the deeper Chl *a* maximum during large part of the

12   cruise, while some profiles were characterized by elevated concentrations in the surface

13   usually associated with upwelling water. Both kinds of profiles are consistent with previous

14   studies finding maxima in the deeper water column in the open ocean and surface maxima in

15   upwelling regions (Yamamoto et al., 2001; Quack et al., 2004; Hepach et al., 2015). During

16   the northern part of M91 (upwelling III), CH_2Br_2 in the water column was more elevated than

17    $CHBr_3$, while during the remaining part of the cruise, $CHBr_3$ was usually higher.

18   Though most of the stations were characterized by subsurface maxima of iodocarbons, which

19   were mostly located between 10 and 50 m (see example in Fig. 4, upper panel), surface

20   maxima were often observed in upwelling region IV (see example in Fig. 4, lower panel), the

21   region with highest iodocarbon concentrations. Profiles with surface maxima were generally

22   characterized by much higher concentrations of these compounds. Similarly to very low

23   CH_2I_2 concentrations in the surface in the northern part of the measurements, it was also

24   hardly detected in the deeper water in this region (Fig. 4, upper panel). Surface maxima in

25   depth profiles of CH_3I and CH_2ClI were connected to surface maxima of several

26   phytoplankton species, mainly diatoms ($r_s = 0.57$ and 0.62). Direct and indirect biological and

27   photochemical formation account as possible sources for these maxima. CH_2I_2 was usually

28   strongly depleted in the surface in contrast to the deeper layers due to its rapid photolysis,

29   which may also have been a source for surface CH_2ClI. Subsurface maxima occurred both

30   below and within the mixed layer (see the example in Fig. 4d indicated by the temperature-,

31   salinity- and density profiles). Maxima in the mixed layer probably appear because of very

32   fast production (Hepach et al., 2015), while maxima below the mixed layer are supported by

33   accumulation due to reduced mixing.

Atmospheric
Chemistry
and Physics
Discussions

1   All five halocarbons were strongly depleted in waters below 50 m. These deeper layers were

2   also characterized by very low oxygen values, known as strong OMZ below the biologically

3   active layers (Karstensen et al., 2008). A possible reason for the strong depletion of the

4   halocarbons is their bacterial mediated reductive dehalogenation occurring under anaerobic

5   conditions (Bouwer et al., 1981; Tanhua et al., 1996).

6

7   **5   Relationship of surface halocarbons to environmental parameters**

8   Physical and chemical parameters as well as biological proxies such as TChl *a* and

9   phytoplankton group composition were investigated using correlation analysis in order to

10 investigate marine sources of halocarbons.

11 **5.1   Potential bromocarbon sources**

12 Bromocarbons were weakly, but significantly anticorrelated with SSS and SST (r_s between -

13 0.29 and -0.57), indicating sources in the upwelled water (Table 2). They showed a positive

14 correlation with diatoms ($r_s = 0.58$ for both compounds), the dominant phytoplankton group in

15 the region. Diatoms have already been found to be involved in bromocarbon production in

16 several laboratory and field studies (Tokarczyk and Moore, 1994; Moore et al., 1996; Quack

17 et al., 2007b; Hughes et al., 2013). Thus, these findings are in agreement with current

18 assumptions that diatoms may contribute directly or indirectly to bromocarbon production.

19 During M91, CH_2Br_2 was more abundant in cooler, nutrient-rich water than $CHBr_3$, leading to

20 a stronger correlation with TChl *a* and SST, indicating an additional source associated with

21 fresh upwelling. No significant correlations were found for bromocarbons with

22 polysaccharidic DOM (Table 3), implying that DOM components analyzed during the cruise

23 were not involved in bromocarbon production, at least not in the upper water column.

24 **5.2   Iodinated compounds and phyotplankton**

25 In general, the iodocarbons correlated stronger with biological parameters than the

26 bromocarbons. Diatoms were found to correlate very strongly with all three iodocarbons ($r_s =$

27 0.73 with CH_3I, $r_s = 0.79$ with CH_2ClI and $r_s = 0.72$). Weak but significant anticorrelations

28 with DIN:DIP and SST suggest that iodocarbons were associated with cool and slightly DIN

29 depleted water. The occurrence of large amounts of iodocarbons seemed to be associated with

30 an established diatom bloom. The production of CH_3I, CH_2ClI and CH_2I_2 by a number of

31 diatom species has been observed in several studies before (Moore et al., 1996; Manley and

Atmospheric
Chemistry
and Physics
Discussions

1   de la Cuesta, 1997), consistent with our findings. The very high correlation of cryptophytes

2   with iodocarbons was likely based on the co-occurrence of these species with diatoms (Table

3   2 and description in section 3).

4   **5.3   Iodinated compounds and DOM**

5   Correlations of the three iodinated compounds to polysaccharidic DOM components in

6   subsurface water revealed a strong relationship of the iodocarbon abundance with

7   polysaccharides and in particular uronic acids (Table 3). CH_3I and CH_2ClI showed strong

8   correlations with particulate uronic acids (both $r_s = 0.84$), total uronic acids ($r_s = 0.83$ and

9   0.88) and dissolved polysaccharides ($r_s = 0.82$ and 0.90). The correlations of CH_2I_2 with

10   polysaccharides were less strong, but significant ($r_s = 0.68$ with particulate, $r_s = 0.66$ with total

11   and $r_s = 0.55$ with dissolved). The above listed DOM components were also significantly

12   correlated to diatoms ($r_s = 0.68$ with polysaccharides and $r_s = 0.75$ with uronic acids), which

13   were a potential source for the accumulated organic matter in the subsurface. The exact

14   composition of surface water DOM is determined by the phytoplankton species producing the

15   DOM. Polysaccharides with uronic acids as an important constituent have for example been

16   shown to contribute largely to the DOM pool in a diatom rich region (Engel et al., 2012).

17   Hill and Manley (2009) tested several diatom species for their production of halocarbons in a

18   laboratory study, and suggested that a major formation pathway for polyhalogenated

19   compounds may actually not be from direct algal production, but rather indirectly through

20   their release of hypoiodous (HOI) and hypobromous acid (HOBr), which then react with the

21   present DOM (Liu et al., 2015). The formation of HOI and HOBr within the algae is

22   enzymatic with possible chloroperoxidase (CPO), BPO and iodoperoxidase (IPO)

23   involvement. While CPO and BPO may produce both HOBr and HOI, IPO only leads to HOI.

24   Moore et al. (1996) suggested that the occurrence of BPO and IPO in the phytoplankton cells

25   may be highly species dependent. This leads to the assumption that diatoms abundant in the

26   Peruvian upwelling contained more IPO than BPO, which could explain the higher abundance

27   of iodocarbons relative to bromocarbons during M91.

28   The formation of CH_3I through DOM may be different than the production of CH_2ClI and

29   CH_2I_2. While CH_2I_2 is suggested to be formed via haloform-type reactions (Carpenter et al.,

30   2005), CH_3I is produced using a methyl-radical source (White, 1982). The relationship of

31   CH_3I with DOM can be the result of both photochemical and biological production pathways:

32   DOM, which was observed in high concentrations in the biologically productive waters, can

Atmospheric
Chemistry
and Physics
Discussions

1   act as the methyl-radical source during photochemical production of CH_3I (Bell et al., 2002).

2   A second possible biological pathway of methyl iodide production takes place via bacteria

3   and micro algae, which can utilize methyl transferases in their cells. HOI plays a significant

4   role in this production pathway by providing the iodine to the methyl group (Yokouchi et al.,

5   2014).

6   In conclusion, the Peruvian upwelling was a strong source for the iodocarbons CH_3I, CH_2ClI

7   and CH_2I_2, and a weaker source for the bromocarbons $CHBr_3$ and CH_2Br_2. We propose a

8   formation mechanism for this region as described in Fig. 5 based on measurements of short-

9   lived halocarbons and biological parameters during M91. Diatoms, which can contain the

10   necessary enzymes for halocarbon formation, were identified as important source based on

11   their strong correlations with the bromo- and iodocarbons and with polysaccharidic DOM.

12   The very good correlations of iodocarbons with polysaccharides and uronic acids are a hint

13   that these DOM components may have been important substrates for iodocarbon production

14   potentially produced from the present diatoms. The higher iodocarbon concentrations can

15   likely be explained by phytoplankton species containing more IPO than BPO, leading to a

16   stronger production of iodocarbons. Additionally, the particular type of DOM may also have

17   regulated the production of specific halocarbons (Liu et al., 2015), in this case CH_3I, CH_2ClI

18   and CH_2I_2.

19   One interesting feature of our analysis is the fact that CH_2I_2 when compared to the other two

20   iodocarbons showed weaker correlations with the polysaccharides possibly due to its shorter

21   surface water lifetime. Moreover, CH_2I_2 and CH_2ClI showed weaker correlations in the

22   Peruvian upwelling than during other cruises in the tropical Atlantic, namely MSM18/3

23   (Hepach et al., 2015) and DRIVE (Hepach et al., 2014). Combining the two arguments of a

24   short CH_2I_2 lifetime and only a weak correlation between CH_2I_2 and CH_2ClI, this may

25   indicate an additional source for CH_2ClI similar to CH_3I, explaining why CH_3I and CH_2ClI

26   correlate much better with each other than with CH_2I_2.

27

28   **6   From the ocean to the atmosphere**

29   **6.1   Sea-to-air fluxes of iodocarbons**

30   Due to high oceanic iodocarbon concentrations measured in sea surface water of the Peruvian

31   upwelling and despite the moderate prevailing wind speeds of 6.17 (0.42 – 15.47) m s^{-1}, high

32   iodocarbon sea-to-air fluxes were calculated in contrast to the rather low bromocarbon

Atmospheric
Chemistry
and Physics
Discussions

1   emissions during this M91 cruise (Fuhlbrügge et al., 2015a). The highest average fluxes of the

2   three iodocarbons of 954 (21 – 4686) were calculated for CH_3I, followed by 834 (-24 – 5652)

3   for CH_2ClI, and finally 504 (-126 – 2546) pmol m^{-2} h^{-1} for CH_2I_2 (Table 1). These were on

4   average 4 to 7 times higher than $CHBr_3$ and 2 to 4 times higher than the CH_2Br_2 sea-to-air

5   fluxes during the cruise.

6   Our estimated fluxes of CH_3I are in the range of emissions calculated for the tropical and

7   subtropical Atlantic of 625 to 2154 pmol m^{-2} h^{-1} (Chuck et al., 2005; Jones et al., 2010).

8   Moore and Groszko (1999), who performed a study between 40° N and 40° S close to our

9   investigation region but not covering the Peruvian upwelling, calculated on average 666 pmol

10 m^{-2} h^{-1}, which is 0.7 times our flux. Sea-to-air fluxes of CH_2ClI from the same studies were

11 reported to range on average between 250 and 1138 pmol m^{-2} h^{-1} with the largest fluxes

12 originating from the Mauritanian upwelling region. These are 0.3 to 1.4 times the fluxes we

13 calculated, showing that the Peruvian upwelling region is at the top end of oceanic CH_2ClI

14 emissions. We are only aware of two studies focusing on emissions of CH_2I_2 from the

15 Atlantic tropical ocean (Jones et al., 2010; Hepach et al., 2015) which are on average 0.2,

16 respectively 1.4 times the fluxes from the tropical East Pacific. The larger sea-to-air fluxes

17 reported in Hepach et al. (2015) from the equatorial Atlantic cold tongue are mainly a result

18 of much lower atmospheric mixing ratios there, increasing the concentration gradient, and

19 additionally higher wind speeds, increasing the exchange coefficient k_w.

20 Summarizing this section, the large production of iodocarbons in the Peruvian upwelling led

21 to enhanced emissions of these compounds to the troposphere despite very low wind speeds.

22 An additional factor influencing halocarbon emissions is the low height and insolation of the

23 MABL, where halocarbons accumulate above the air-sea interface. The large sea-to-air fluxes

24 and low wind speeds should result in high tropospheric iodocarbons, which was indeed

25 observed and is discussed in the following section.

26 **6.2   Atmospheric iodocarbons**

27 Atmospheric mixing ratios of the three iodocarbons were elevated during M91 with up to 3.2

28 ppt for CH_3I, up to 2.5 ppt for CH_2ClI and up to 3.3 ppt for CH_2I_2 (Table 1), likely a result of

29 the strong production and emissions of these compounds.

30 CH_3I data were generally elevated in comparison to other eastern Pacific measurements of up

31 to 2.1 ppt CH_3I (Butler et al., 2007), but lower than in the tropical central and East Atlantic

32 around the equator, characterized by higher atmospheric CH_3I of over 5 ppt (Ziska et al.,

1   2013). Both CH_2ClI and CH_2I_2 were also elevated in comparison to previous oceanic

2   measurements, where e.g. 0.01 to 0.99 ppt CH_2ClI were measured for remote locations in the

3   Atlantic and Pacific (Chuck et al., 2005; Varner et al., 2008) and only up to 0.07 ppt were

4   reported for CH_2I_2 at a remote site in the Pacific (Yokouchi et al., 2011). Coastal areas with

5   high macroalgal abundance were characterized by high CH_2ClI of up to 3.4 ppt (Varner et al.,

6   2008) and up to 3.1 ppt CH_2I_2 (Carpenter et al., 1999; Peters et al., 2005), while 19.8 ppt

7   (Peters et al., 2005) were measured at Mace Head, Ireland and Lilia, Brittany in the North

8   Atlantic.

9   The different atmospheric lifetimes of the three iodocarbons, ranging between 4 d (CH_3I), 9 h

10 (CH_2ClI) and 10 min (CH_2I_2) (Carpenter and Reimann, 2014), partly explain the observed

11 differences in their distributions. Although atmospheric CH_3I was generally elevated in

12 regions of high oceanic CH_3I (Fig. 3) in upwelling regions III and IV, the atmospheric and

13 oceanic data did not show a significant correlation. The CH_3I lifetime of several days allows

14 atmospheric CH_3I to mix within the MABL, possibly masking a correlation between local

15 source regions and elevated mixing ratios.

16 The two shorter-lived iodinated compounds CH_2ClI and CH_2I_2 generally showed a stronger

17 influence of local marine sources. Both species correlate significantly with their oceanic

18 concentrations with $r_s = 0.60$ (CH_2ClI) and $r_s = 0.64$ (CH_2I_2). Oceanic CH_2ClI and CH_2I_2 were

19 emitted into the boundary layer where they could accumulate during night (see comparison

20 with global radiation in Fig. 3b), and were rapidly degraded during day time via photolysis,

21 which is their main sink in the troposphere (Carpenter and Reimann, 2014). Moderate average

22 wind speeds in the upwelling regions (Fig. 6) and stable atmospheric boundary layer

23 conditions (Fuhlbrügge et al., 2015a) supported the accumulation of these compounds.

24 The Peruvian upwelling was in general characterized by elevated atmospheric iodocarbons as

25 a result of their large sea-to-air fluxes caused by strong biological production. The upwelling

26 could sustain elevated atmospheric levels of e.g. CH_3I, could trap iodocarbons and their

27 degradation products in a stable MABL, and may have therefore contributed significantly to

28 the tropospheric inorganic iodine budget, which is discussed in the following.

29 **6.3   Contributions to tropospheric iodine**

30 After their emission from the ocean and their chemical degradation in the marine boundary

31 layer, iodocarbons contribute to the atmospheric inorganic iodine budget, I_y. The importance

32 of this contribution compared to abiotic sources is currently under debate and analyzed for

Atmospheric
Chemistry
and Physics
Discussions

1   various oceanic environments (Mahajan et al., 2010; Grossmann et al., 2013; Prados-Roman

2   et al., 2015). So far, no correlations of IO with the organic iodine precursor species have been

3   observed (Grossmann et al., 2013) and correlations between IO and Chl *a* were often found to

4   be negative (Mahajan et al., 2012; Gómez Martín et al., 2013). Chemical modelling studies,

5   undertaken to explain the contributions of organic and inorganic oceanic iodine sources,

6   simulated that only a small fraction of the atmospheric IO stems from the organic precursors

7   with estimates of about 25 % on a global average (Prados-Roman et al., 2015). Both

8   arguments, the missing correlations and the small contributions, indicate that the organic

9   source gas emissions play a minor role for the atmospheric iodine budget. Given the special

10 conditions of the Peruvian upwelling with cold nutrient rich waters, the strong iodocarbon

11 sources and a stable MABL and trade inversion, it is of interest to analyze the local

12 contributions to the atmosphere in this region and to compare with estimates from other

13 oceanic environments.

14 We focus our analysis on the section of the cruise where MAX-DOAS measurements of IO

15 and simultaneous iodocarbon measurements in the surface water and atmosphere were made

16 (roughly south of 10° S). Tropospheric VCDs of IO in the range of $2.5 - 6.0 \times 10^{12}$ molec cm^{-2}

17 were inferred from the MAX-DOAS measurements. Similar VCDs of IO were reported by

18 Schönhardt et al. (2008) based on remote satellite measurements from SCIAMACHY.

19 Volume mixing ratios of IO along the cruise track (Fig. 7a) derived from the MAX-DOAS

20 measurements show a pronounced variability and maxima close to upwelling regions II and

21 IV. Daytime averaged IO volume mixing ratios are displayed in Fig. 7b and range between

22 0.8 ppt (on December 12 and December 22) and 1.5 ppt (on December 26). Overall the

23 daytime IO abundance in the MABL above the Peruvian upwelling was relatively high

24 compared to measurements from the nearby Galapagos islands (~ 0.4 ppt) (Gómez Martín et

25 al., 2013) and from other tropical oceans such as the Malaspina 2010 circumnavigation (0.4 –

26 1 ppt) (Prados-Roman et al., 2015). Other measurement campaigns such as the Cape Verde

27 measurements (Read et al., 2008) or the TransBrom Sonne in the West Pacific (Grossmann et

28 al., 2013) found similar IO mixing ratios with values above 1 ppt, but significantly lower IO

29 VCDs in case of the latter.

30 The M91 cruise track crisscrossed the waters between the coast and 200 km offshore multiple

31 times, providing a comprehensive set of measurements over a confined area (see Fig. 7a) and

32 allowing us to analyze the relation between IO and organic precursors. Assuming constant

33 emissions over the cruise period we can link the oceanic sources with atmospheric IO

34 observations at locations reached after hours to days of atmospheric transport. Therefore, we

Atmospheric
Chemistry
and Physics
Discussions

1   released FLEXPART trajectories from all sea surface measurement locations continuously

2   over the whole measurement time period from December 8 to December 26 loaded with the

3   oceanic organic iodine as prescribed by the observed iodocarbon emissions. Based on the

4   simulations of transport and chemical decay described in Section 2.5, we derived organic and

5   inorganic iodine mixing ratios individually for each air parcel. Mixing with air parcels

6   impacted by other source regions was not taken into account. FLEXPART-based IO

7   originating from organic precursors was derived as mean values over all air parcels in the

8   MABL coinciding with the MAX-DOAS measurement locations within an area of 5 km x 5

9   km. Simplifying assumptions of a prescribed inorganic iodine lifetime (2 days) and IO to I_y

10   ratio (0.15 to 0.3) were made to derive the IO mixing ratios. Uncertainties were estimated

11   based on additional runs with varying atmospheric lifetime of inorganic iodine $(1 - 3$ days).

12   For the first part of the cruise from December 8 to December 18, FLEXPART-derived IO

13   mixing ratio estimates at the MAX-DOAS measurement locations (red line in Fig. 7b and c)

14   explain between 40 and 70 % (55 % on average) of the measured IO assuming a lifetime for

15   inorganic iodine of 2 days. As a consequence, about 0.5 ppt of IO is expected to originate

16   from other, likely inorganic, iodine sources. For the scenario of a shorter I_y lifetime (one day),

17   we find that the organic sources explain about 30 % of the IO and for a relatively long

18   lifetime (three days), 80 % can be explained. In general, the air masses were transported along

19   the coast in northwest direction and organic sources contribute to the IO budget along this

20   transport path. Most of the IO results from CH_2ClI (Fig. 7c) which was transported some

21   hours northwestwards (lifetime of 9 hours) before contributing to the atmospheric inorganic

22   iodine budget.

23   For the second part of the cruise from December 19 to December 26, the amount of IO

24   estimated from organic precursors was much smaller and often close to zero. This very small

25   organic contribution was caused by two facts. First, the instantaneous sources during the last

26   part of the cruise were much smaller (Fig. 6b – d) and second, further southward situated

27   sources, which also influence the iodine abundance in the cruise track region were not

28   analyzed and thus not included in the simulations. Because of missing information on the

29   source strength and distribution southwards of the cruise track, a proper comparison is only

30   possible for the first part of the cruise before December 19. However, given that the MAX-

31   DOAS measurements of IO remained relatively high during the second part of the cruise, it is

32   likely that additional significant organic iodine sources existed further southwards. This

33   assumption is also supported by the fact that atmospheric CH_3I mixing ratios remained

34   relatively high during the second part of the cruise (50 % compared to the earlier part, see Fig.

Atmospheric
Chemistry
and Physics
Discussions

1   3b) while the water concentrations were close to zero. Consequently, a source region of CH_3I

2   must have existed further southwards contributing to the observed mixing ratios of CH_3I and

3   IO after some hours to days of atmospheric transport.

4   While the contribution of organic iodine to IO during the first part of the cruise is

5   considerably higher than found in other regions, the amount of inorganic iodine precursors of

6   0.5 ppt necessary to explain total IO is very similar to the one derived in other studies

7   (Prados-Roman et al., 2015). The higher organic contribution was consistent with the fact that

8   there was an overall higher IO abundance compared to most other campaigns. Instantaneous

9   IO and organic source gas emissions during M91 were not directly correlated. However,

10   taking the transport within the first hours and days into account enables us to explain a

11   considerable part of the atmospheric IO variations with the variability of the oceanic organic

12   sources (Fig. 7b). Overall, we conclude that for the Peruvian upwelling region with special

13   conditions in the ocean and atmosphere, higher iodocarbon sources lead to larger IO

14   abundances while the absolute inorganic contribution is similar to other regions.

15

16   **7   Conclusions**

17   The Peruvian upwelling at the west coast of South America was characterized for halocarbons

18   for the first time during the M91 cruise. We measured moderate concentrations of the

19   bromocarbons $CHBr_3$ and CH_2Br_2, while we observed exceptionally high concentrations of

20   the iodocarbons CH_3I, CH_2ClI and CH_2I_2 in the surface seawater.

21   $CHBr_3$ and CH_2Br_2 were significantly correlated with TChl *a* and diatoms, suggesting

22   biological formation of these compounds. Higher correlations of diatoms were found with the

23   three iodocarbons, and even stronger correlations of the iodocarbons with the DOM

24   components polysaccharides and uronic acids were observed. The polyhalogenated

25   compounds CH_2ClI and CH_2I_2 were potentially formed via these DOM components with the

26   likely involvement of diatoms. CH_3I may have been formed via photochemistry from the

27   large pool of observed DOM and/or biologically via methyl transferases in micro algae and

28   bacteria. The production of iodocarbons from DOM via the proposed mechanisms seems to

29   have exceeded the bromocarbon production in the region in contrast to several previous

30   studies in tropical Atlantic upwelling regions (Hepach et al., 2014, 2015).

31   Depth profiles showed subsurface maxima, common in the open ocean, and very pronounced

32   and elevated surface maxima in regions of highest underway iodocarbon concentrations. The

Atmospheric
Chemistry
and Physics
Discussions

1   surface water was always depleted in CH_2I_2 with respect to the underlying water column due

2   to its very rapid photolysis. The OMZ at depth was strongly depleted in all five measured

3   halocarbons, suggesting an effective sink in the oxygen depleted waters.

4   The high oceanic iodocarbon concentrations and elevated emissions also led to elevated

5   atmospheric mixing ratios in the marine boundary layer. Atmospheric CH_2ClI and CH_2I_2

6   showed clear diurnal cycles, accumulating during night and decreasing rapidly during day

7   time. Despite previous suggestions that the tropospheric iodine loading is mainly a product

8   from direct emission of HOI and I_2, we calculated important contributions of iodocarbons to

9   the observed IO levels. Using FLEXPART, we estimated a contribution of combined

10 iodocarbon fluxes to IO of 30 to 80 % assuming an inorganic iodine lifetime between 1 and 3

11 days. This contribution of organoiodine is much higher than previously assumed (Prados-

12 Roman et al., 2015), suggesting that iodocarbons therefore may contribute significantly to

13 tropospheric iodine levels in regions of strong iodocarbon production mediated by

14 phytoplankton (diatoms) and bacteria.

15 Our observations reveal several uncertainties which need to be addressed in the future to

16 better constrain the halocarbon budget and understand its role in a changing climate. Further

17 studies of upwelling regions need to be performed in different seasons and years, since these

18 regions are impacted by synoptic and climatic conditions, which are expected to have an

19 impact on the strength of halocarbon emissions. A regular monitoring and better knowledge

20 of halocarbon sources and emissions is severely needed, since these have numerous

21 implications for atmospheric processes such as ozone chemistry and aerosol formation, which

22 have been investigated in several atmospheric modeling studies. These studies have mostly

23 applied Chl *a* as proxy for halocarbon emissions. However, the potential involvement of

24 DOM in the production of both iodo- and bromocarbons and the often weak correlation to Chl

25 *a* in the field raises the question whether Chl *a* is a suitable parameter to estimate halocarbon

26 concentrations. Laboratory studies are therefore crucial to help identifying more adequate

27 parameters for predicting halocarbons in the ocean. Associated with the involvement of DOM

28 in iodocarbon production is the occurrence of the relevant DOM components in large

29 concentrations in the sea surface microlayer (SML) (Engel and Galgani, 2015). The SML has

30 been shown to cover a wide range of oceanic regions (Wurl et al., 2011), which could

31 represent a significant additional source to atmospheric iodocarbons. The potential of the

32 SML to produce CH_2I_2 has been previously suggested by Martino et al. (2009), who proposed

33 that HOI converted from iodide in the SML may react with the present DOM, which may

34 apply to CH_2ClI and CH_3I as well. Furthermore, the SML is in direct contact to the

Atmospheric
Chemistry
and Physics
Discussions

Open Access

EGU

1 atmosphere, and the direct exposure to light may enhance halocarbon emissions (see also Fig.

2 5). The influence of these halocarbon emissions on the tropospheric halogen loading is still

3 very much under debate, and our results underline the importance to constrain the actual

4 contribution of these compounds to tropospheric halogen chemistry.

5

6 **Acknowledgements**

14

15

16

17

18

19

20

21

22

23

24

25

26

27

28

29

Atmospheric
Chemistry
and Physics
Discussions

Open Access

EGU

1 **Tables**

2 Table 1. Environmental parameters, as well as halocarbons in water, air and sea-to-air fluxes

3 during the cruise. Means of sea surface temperature (SST), sea surface salinity (SSS) and

4 wind speed are for 10-min-averages.

Parameter		Unit	Mean (min - max)
SST		°C	19.4 (15.0 - 22.4)
SSS			34.95 (34.10 - 35.50)
TChl a		$\mu g\ L^{-1}$	1.80 (0.06 - 12.65)
Wind speed		$m\ s^{-1}$	6.17 (0.42 - 15.47)
CHBr$_3$	Water	$pmol\ L^{-1}$	6.6 (0.2 - 21.5)
	Air	ppt	2.9 (1.5 - 5.9)
	Sea-to-air flux	$pmol\ m^{-2}\ h^{-1}$	130 (-550 - 2201)
CH$_2$Br$_2$	Water	$pmol\ L^{-1}$	4.3 (0.2 - 12.7)
	Air	ppt	1.3 (0.8 - 2.0)
	Sea-to-air flux	$pmol\ m^{-2}\ h^{-1}$	273 (-128 - 1321)
CH$_3$I	Water	$pmol\ L^{-1}$	9.8 (1.1 - 35.4)
	Air	ppt	1.5 (0.6 - 3.2)
	Sea-to-air flux	$pmol\ m^{-2}\ h^{-1}$	954 (21 - 4686)
CH$_2$ClI	Water	$pmol\ L^{-1}$	10.9 (0.4 - 58.1)

22

Atmospheric
Chemistry
and Physics

Open Access

EGU

Discussions

	Air	ppt	0.4 (0 - 2.5)
	Sea-to-air flux	pmol m^{-2} h^{-1}	834 (-28 - 5652)
	Water	pmol L^{-1}	7.7 (0.2 - 32.4)
CH_2I_2	Air	ppt	0.2 (0 - 3.3)
	Sea-to-air flux	pmol m^{-2} h^{-1}	504 (-126 - 2546)

Atmospheric
Chemistry
and Physics
Discussions

Open Access

EGU

1 Table 2. Spearman's rank correlation coefficients of correlations of halocarbon with several ambient parameters, as well as biological proxies.
2 Bold numbers indicate correlations that are significant with $p < 0.05$ with a sample number of 107 for all environmental data and 46 for all
3 phytoplankton and nutrient data considering all collocated surface data.

	$CHBr_3$	CH_2Br_2	CH_3I	CH_2ClI	CH_2I_2	SST	SSS	Global radiation	Diatoms	Crypto-phytes	Dino-flagellates	TChl a
DIN:DIP	-0.26	-0.34	**-0.38**	**-0.30**	-0.32	0.00	**0.41**	0.13	-0.18	-0.17	-0.10	-0.08
TChl a	**0.48**	**0.56**	**0.73**	**0.74**	**0.70**	**-0.82**	**-0.77**	-0.20	**0.93**	**0.85**	**0.33**	
Dino-flagellates	0.15	0.28	0.15	0.17	0.21	-0.23	-0.22	-0.01	**0.38**	0.26		
Crypto-phytes	**0.38**	**0.54**	**0.61**	**0.61**	**0.64**	**-0.74**	**-0.79**	-0.18	**0.73**			
Diatoms	**0.58**	**0.58**	**0.73**	**0.79**	**0.72**	**-0.76**	**-0.72**	-0.18				
Global radiation	0.14	-0.10	-0.22	-0.03	-0.08	**0.20**	0.12					
SSS	**-0.44**	**-0.48**	**-0.75**	**-0.69**	**-0.45**	**0.68**						
SST	**-0.29**	**-0.57**	**-0.52**	**-0.62**	**-0.58**							
CH_2I_2	**0.60**	0.43	**0.66**	**0.59**								
CH_2ClI	**0.64**	**0.70**	**0.83**									
CH_3I	**0.66**	**0.46**										

Atmospheric
Chemistry
and Physics

Open Access

EGU

Discussions

CH_2Br_2 **0.56**

Atmospheric
Chemistry
and Physics
Discussions

1 Table 3. Correlations of halocarbons with combined high molecular weight (HMW)

2 carbohydrates (CCHO) and uronic acids (URA) from subsurface samples (T – total, d –

3 dissolved, P – particulate) with a sample number of 29 for each variable.

	$CHBr_3$	CH_2Br_2	CH_3I	CH_2ClI	CH_2I_2
TCCHO	0.15	0.28	**0.78**	**0.82**	**0.66**
dCCHO	0.39	0.48	**0.82**	**0.90**	**0.55**
PCCHO	-0.06	-0.10	**0.61**	**0.64**	**0.68**
TURA	0.31	0.34	**0.83**	**0.88**	**0.52**
dURA	-0.18	0.42	**0.48**	**0.79**	**0.50**
PURA	0.37	0.22	**0.84**	**0.84**	**0.54**

4

5

6

7

8

9

10

11

12

13

14

15

16

17

18

19

20

Atmospheric
Chemistry
and Physics
Discussions

Open Access

1   **Figures**
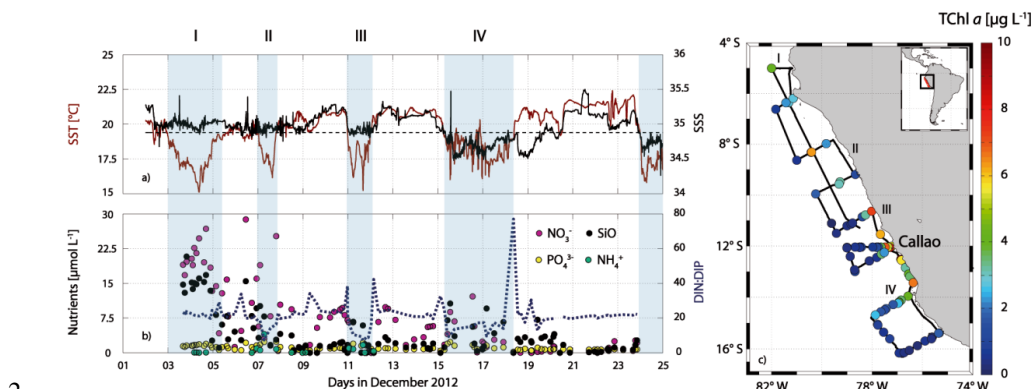
3   Fig. 1. Ambient parameters during the M91 cruise: SST (dark red) and sea surface salinity

4   (SSS) (black) in a) with the dashed line as the mean SST. Nutrients (purple is nitrate – NO_3^-,

5   yellow is phosphate – PO_4^{3-}, black is silicate – SiO_2, light cyan is ammonium – NH_4^+) with

6   the N to P ratio (dark blue dashed line) are shown in b). Total chlorophyll a (TChl a) is shown

7   in the map in c). The light blue shaded areas stand for the regions where SST is below the

8   mean, indicating upwelling of cold water.

Atmospheric
Chemistry
and Physics
Discussions

Open Access

EGU

1
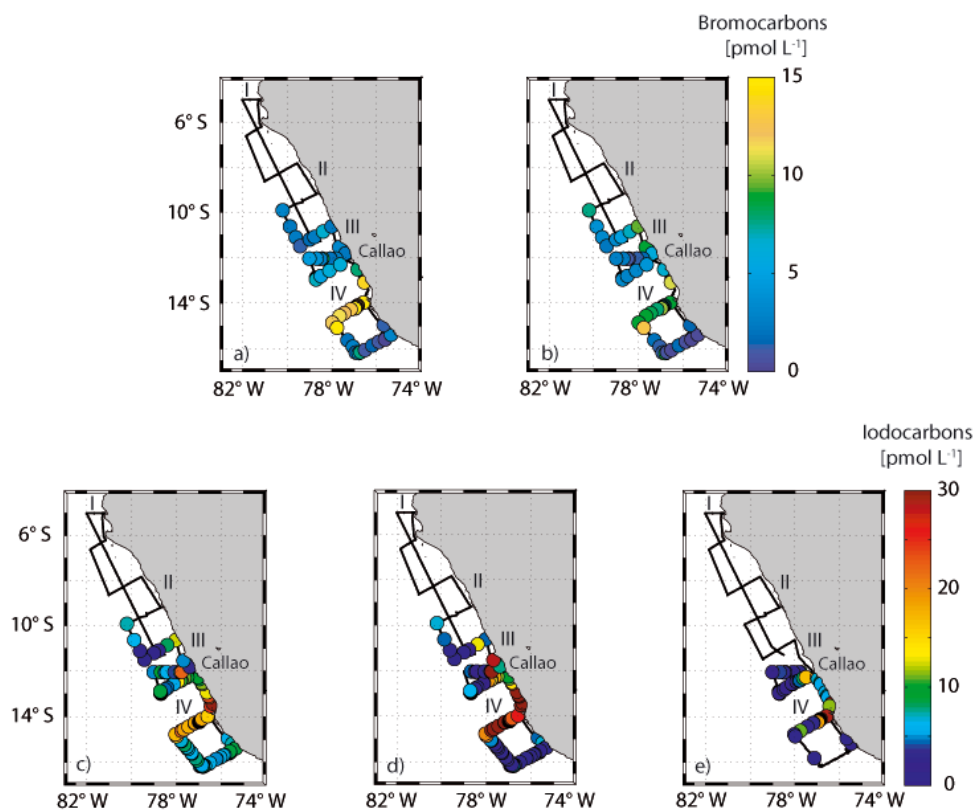
1   Fig. 2. Halocarbon surface water measurements are shown in a) and b) for the bromocarbons

2   (note the colorbar oin the upper panel) with a – $CHBr_3$ and b – CH_2Br_2. Iodocarbons can be

3   found in c) – e) (note the colorbar in the lower panel) with c – CH_3I, d – CH_2ClI and e –
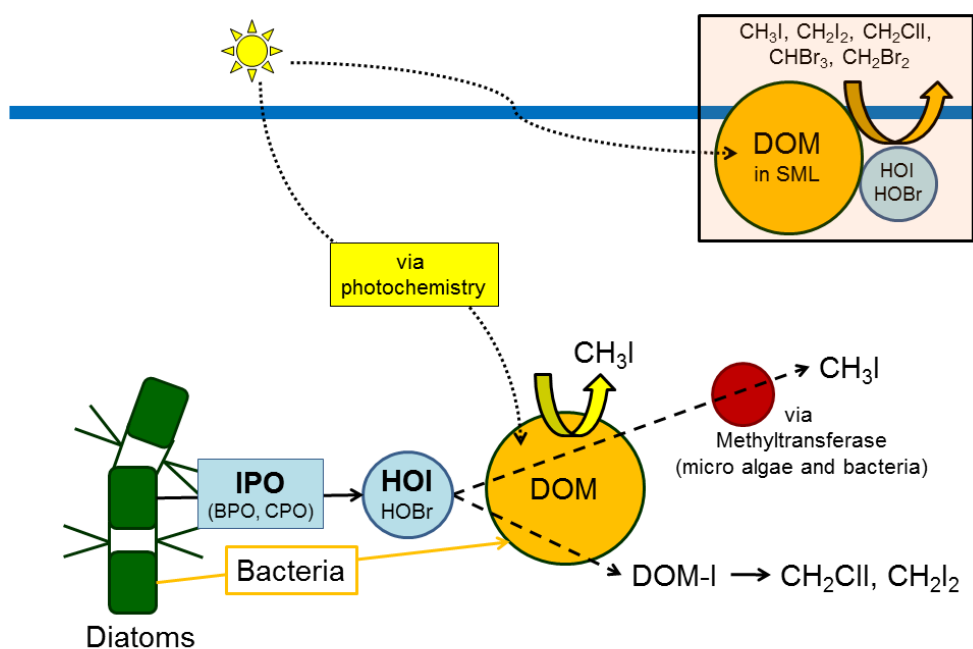
4   CH_2I_2.

5
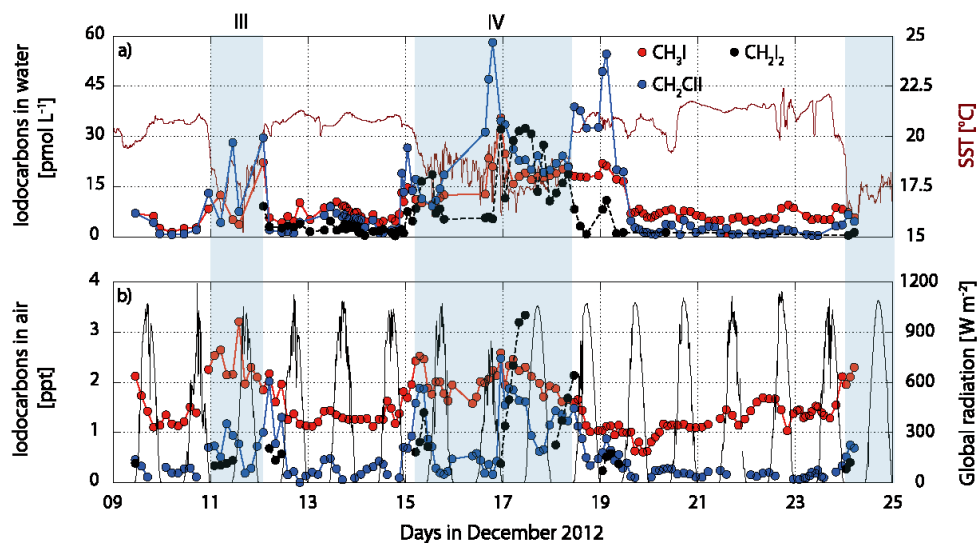
6

7   Fig. 3. Surface water measurements of iodocarbons are presented in a) with CH_3I in red,

8   CH_2ClI in blue and CH_2I_2 in black on the left side along with SST (dark red) on the right side.

9   Additionally, atmospheric mixing ratios of CH_3I (red), CH_2ClI (blue) and CH_2I_2 (grey) on the

10   left side together with global radiation (black) on the right side are depicted in b). Note that all

11   times are in UTC.

12

Atmospheric
Chemistry
and Physics
Discussions

Open Access
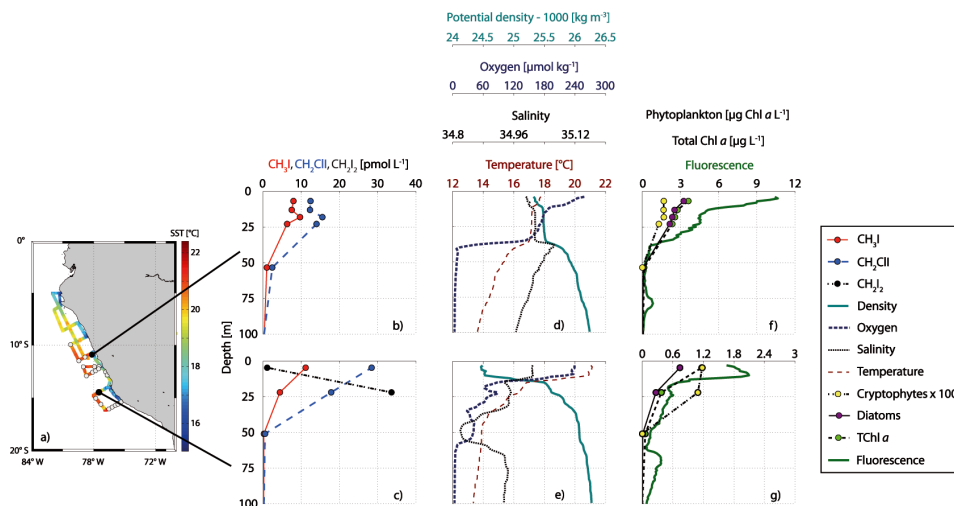
1

2 Fig. 4. A cruise map including all CTD stations and SST is shown in a), while selected depth

3 profiles of iodocarbons can be seen in a) – b), together with ambient parameters such as

4 potential density (cyan), oxygen (dark blue), salinity (black) and temperature (dark red) in d)

5 – e), as well as phytoplankton groups (cryptophytes and diatoms), total chlorophyll a and

6 fluorescence in f) – g). CH_2I_2 was undetectable at the first station (see also consistence with

7 surface data).

8

Atmospheric
Chemistry
and Physics

Discussions

Open Access

EGU

1

2   Fig. 5. Proposed mechanisms for formation of iodocarbons – release of HOI with the help

3   ofvia iodoperoxiases (IPO) and reaction with DOM (dissolved organic matter (DOM) via

4   iodine binding to DOM (DOM-I) to form CH_2ClI and CH_2I_2. CH_3I formation via

5   photochemistry and/or biological formation via methyltransferases. The box indicates

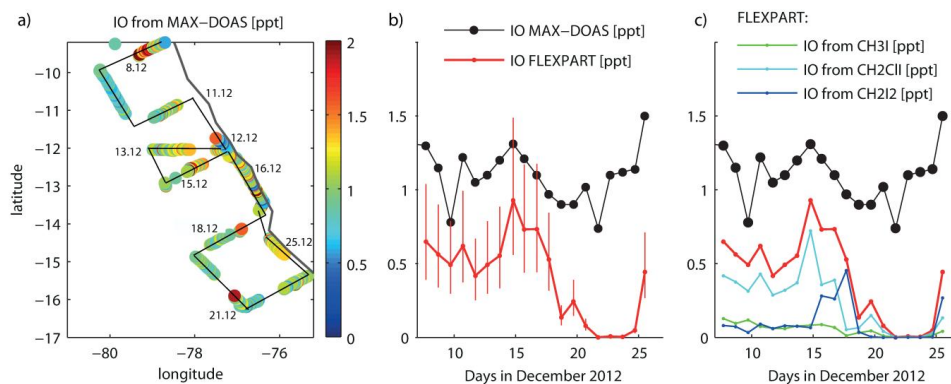6   potential formation of halocarbons from DOM in the sea surface microlayer SML.

7

Atmospheric
Chemistry
and Physics
Discussions
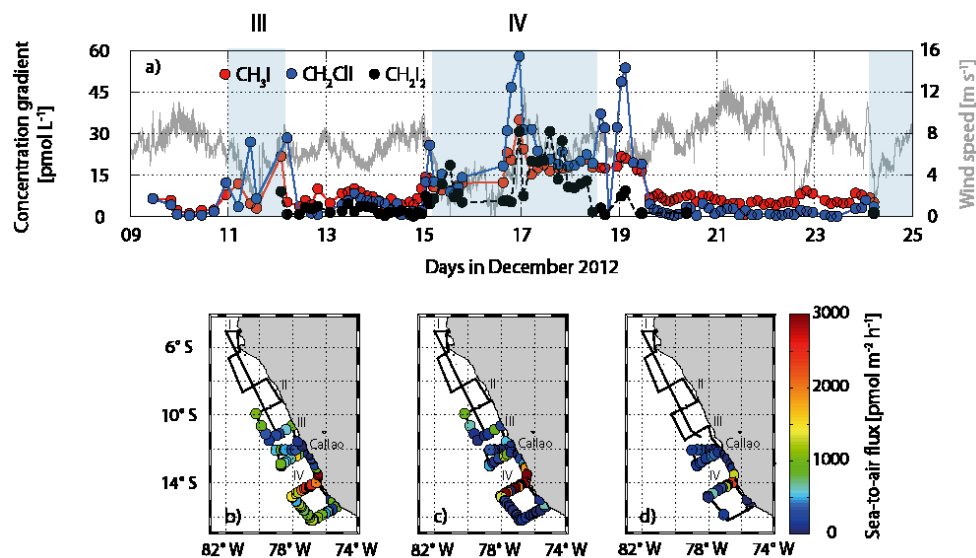
1

2   Fig. 6. The concentration gradient of CH_3I, CH_2ClI and CH_2I_2 along with wind speed (grey) is

3   shown in a), while the sea-to-air flux is depicted in b) for CH_3I, c) for CH_2ClI and d) for

4   CH_2I_2. Note the color bar on the right.

5

6

7   Fig. 7. MAX-DOAS measurements of IO during the M91 campaign along the cruise track are

8   shown a). Daytime averaged IO values from MAX-DOAS and coincident FLEXPART values

9   are provided in b). The vertical bars correspond to uncertainties associated with the inorganic

10 iodine lifetime in the MABL ($1 - 3$ days) and the daytime fraction of IO to I_y (0.15 to 0.3).

Atmospheric Chemistry and Physics Discussions

1   Contributions of the three oceanic iodocarbon sources to the modelled FLEXPART IO are

2   also given in c).

3

4

5

6

7

Atmospheric
Chemistry
and Physics
Discussions

1 References

2 Abrahamsson, K., Lorén, A., Wulff, A., and Wangberg, S. A.: Air-sea exchange of
3 halocarbons: the influence of diurnal and regional variations and distribution of pigments,
4 Deep-Sea Res. Part II-Top. Stud. Oceanogr., 51, 2789-2805, 10.1016/j.dsr2.2004.09.005,
5 2004.

6 Amachi, S., Kamagata, Y., Kanagawa, T., and Muramatsu, Y.: Bacteria mediate methylation
7 of iodine in marine and terrestrial environments, Applied and Environmental Microbiology,
8 67, 2718-2722, 10.1128/aem.67.6.2718-2722.2001, 2001.

9 Amachi, S.: Microbial contribution to global iodine cycling: volatilization, accumulation,
10 reduction, oxidation, and sorption of iodine, Microbes Environ., 23, 269-276,
11 10.1264/jsme2.ME08548, 2008.

12 Archer, S. D., Goldson, L. E., Liddicoat, M. I., Cummings, D. G., and Nightingale, P. D.:
13 Marked seasonality in the concentrations and sea-to-air flux of volatile iodocarbon
14 compounds in the western English channel, J. Geophys. Res.-Oceans, 112,
15 10.1029/2006jc003963, 2007.

16 Bakun, A., and Weeks, S. J.: The marine ecosystem off Peru: what are the secrets of its
17 fishery productivity and what might its future hold?, Prog. Oceanogr., 79, 290-299,
18 http://dx.doi.org/10.1016/j.pocean.2008.10.027, 2008.

19 Bange, H. W.: Surface ocean - lower atmosphere study (solas) in the upwelling region of
20 Peru, Bremerhaven, 69, 2013.

21 Barlow, R. G., Cummings, D. G., and Gibb, S. W.: Improved resolution of mono- and divinyl
22 chlorophylls a and b and zeaxanthin and lutein in phytoplankton extracts using reverse phase
23 c-8 hplc, Marine Ecology Progress Series, 161, 303-307, 10.3354/meps161303, 1997.

24 Bell, N., Hsu, L., Jacob, D. J., Schultz, M. G., Blake, D. R., Butler, J. H., King, D. B., Lobert,
25 J. M., and Maier-Reimer, E.: Methyl iodide: atmospheric budget and use as a tracer of marine
26 convection in global models, J. Geophys. Res.-Atmos., 107, 434010.1029/2001jd001151,
27 2002.

28 Bouwer, E. J., Rittmann, B. E., and McCarty, P. L.: Anaerobic degradation of halogenated 1-
29 and 2-carbon organic compounds, Environ. Sci. Technol., 15, 596-599, 10.1021/es00087a012,
30 1981.

Atmospheric
Chemistry
and Physics
Discussions

1   Brownell, D. K., Moore, R. M., and Cullen, J. J.: Production of methyl halides by
2   prochlorococcus and synechococcus, Glob. Biogeochem. Cycles, 24, GB2002,
3   10.1029/2009gb003671, 2010.

4   Bruland, K. W., Rue, E. L., Smith, G. J., and DiTullio, G. R.: Iron, macronutrients and diatom
5   blooms in the Peru upwelling regime: brown and blue waters of Peru, Mar. Chem., 93, 81-
6   103, 10.1016/j.marchem.2004.06.011, 2005.

7   Burkholder, J. B., Curtius, J., Ravishankara, A. R., and Lovejoy, E. R.: Laboratory studies of
8   the homogeneous nucleation of iodine oxides, Atmos. Chem. Phys., 4, 19-34, 10.5194/acp-4-
9   19-2004, 2004.

10 Butler, J. H., King, D. B., Lobert, J. M., Montzka, S. A., Yvon-Lewis, S. A., Hall, B. D.,
11 Warwick, N. J., Mondeel, D. J., Aydin, M., and Elkins, J. W.: Oceanic distributions and
12 emissions of short-lived halocarbons, Glob. Biogeochem. Cycles, 21, Gb1023

13 10.1029/2006gb002732, 2007.

14 Carpenter, L. J., Sturges, W. T., Penkett, S. A., Liss, P. S., Alicke, B., Hebestreit, K., and
15 Platt, U.: Short-lived alkyl iodides and bromides at Mace Head, Ireland: links to biogenic
16 sources and halogen oxide production, J. Geophys. Res.-Atmos., 104, 1679-1689, 1999.

17 Carpenter, L. J., Hopkins, J. R., Jones, C. E., Lewis, A. C., Parthipan, R., Wevill, D. J.,
18 Poissant, L., Pilote, M., and Constant, P.: Abiotic source of reactive organic halogens in the
19 sub-arctic atmosphere?, Environ. Sci. Technol., 39, 8812-8816, 10.1021/es050918w, 2005.

20 Carpenter, L. J., Jones, C. E., Dunk, R. M., Hornsby, K. E., and Woeltjen, J.: Air-sea fluxes of
21 biogenic bromine from the tropical and north Atlantic ocean, Atmos. Chem. Phys., 9, 1805-
22 1816, 10.5194/acp-9-1805-2009, 2009.

23 Carpenter, L. J., MacDonald, S. M., Shaw, M. D., Kumar, R., Saunders, R. W., Parthipan, R.,
24 Wilson, J., and Plane, J. M. C.: Atmospheric iodine levels influenced by sea surface emissions
25 of inorganic iodine, Nat. Geosci., 6, 108-111, 10.1038/ngeo1687, 2013.

26 Carpenter, L. J., and Reimann, S.: Ozone-depleting substances (odss) and other gases of
27 interest to the montreal protocol, chapter 1 in scientific assessment of ozone depletion, World
28 Meteorological Institution (WMO), Geneva, Report No. 55, 2014.

Atmospheric
Chemistry
and Physics
Discussions

Open Access

EGU

1 Chavez, F. P., Bertrand, A., Guevara-Carrasco, R., Soler, P., and Csirke, J.: The northern

2 humboldt current system: brief history, present status and a view towards the future, Prog.

3 Oceanogr., 79, 95-105, http://dx.doi.org/10.1016/j.pocean.2008.10.012, 2008.

4 Chuck, A. L., Turner, S. M., and Liss, P. S.: Oceanic distributions and air-sea fluxes of

5 biogenic halocarbons in the open ocean, J. Geophys. Res.-Oceans, 110, C10022

6 10.1029/2004jc002741, 2005.

7 Clémer, K., Van Roozendael, M., Fayt, C., Hendrick, F., Hermans, C., Pinardi, G., Spurr, R.,

8 Wang, P., and De Mazière, M.: Multiple wavelength retrieval of tropospheric aerosol optical

9 properties from maxdoas measurements in Beijing, Atmos. Meas. Tech., 3, 863-878,

10 10.5194/amt-3-863-2010, 2010.

11 Czeschel, R., Stramma, L., Weller, R. A., and Fischer, T.: Circulation, eddies, oxygen, and

12 nutrient changes in the eastern tropical south Pacific ocean, Ocean Sci., 11, 455-470,

13 10.5194/os-11-455-2015, 2015.

14 Dee, D. P., Uppala, S. M., Simmons, A. J., Berrisford, P., Poli, P., Kobayashi, S., Andrae, U.,

15 Balmaseda, M. A., Balsamo, G., Bauer, P., Bechtold, P., Beljaars, A. C. M., van de Berg, L.,

16 Bidlot, J., Bormann, N., Delsol, C., Dragani, R., Fuentes, M., Geer, A. J., Haimberger, L.,

17 Healy, S. B., Hersbach, H., Hólm, E. V., Isaksen, L., Kållberg, P., Köhler, M., Matricardi, M.,

18 McNally, A. P., Monge-Sanz, B. M., Morcrette, J. J., Park, B. K., Peubey, C., de Rosnay, P.,

19 Tavolato, C., Thépaut, J. N., and Vitart, F.: The era-interim reanalysis: configuration and

20 performance of the data assimilation system, Quarterly Journal of the Royal Meteorological

21 Society, 137, 553-597, 10.1002/qj.828, 2011.

22 Dix, B., Baidara, S., Bresch, J. F., Hall, S. R., Schmidt, K. S., Wang, S. Y., and Volkamer, R.:

23 Detection of iodine monoxide in the tropical free troposphere, Proc. Natl. Acad. Sci. U. S. A.,

24 110, 2035-2040, 10.1073/pnas.1212386110, 2013.

25 Echevin, V., Aumont, O., Ledesma, J., and Flores, G.: The seasonal cycle of surface

26 chlorophyll in the Peruvian upwelling system: a modelling study, Prog. Oceanogr., 79, 167-

27 176, 10.1016/j.pocean.2008.10.026, 2008.

28 Engel, A., and Handel, N.: A novel protocol for determining the concentration and

29 composition of sugars in particulate and in high molecular weight dissolved organic matter

30 (hmw-dom) in seawater, Mar. Chem., 127, 180-191, 10.1016/j.marchem.2011.09.004, 2011.

Atmospheric
Chemistry
and Physics
Discussions

1   Engel, A., and Galgani, L.: The organic sea surface microlayer in the upwelling region off

2   Peru and implications for air-sea exchange processes, Biogeosciences Discuss., 12, 10579-

3   10619, 10.5194/bgd-12-10579-2015, 2015.

4   Frieß, U., Monks, P. S., Remedios, J. J., Rozanov, A., Sinreich, R., Wagner, T., and Platt, U.:

5   Max-doas o4 measurements: a new technique to derive information on atmospheric aerosols:

6   2. modeling studies, Journal of Geophysical Research: Atmosphere, 111, D14203,

7   10.1029/2005JD006618,, 2006.

8   Fuhlbrügge, S., Quack, B., Atlas, E., Fiehn, A., Hepach, H., and Krüger, K.: Meteorological

9   constraints on oceanic halocarbons above the Peruvian upwelling, Atmos. Chem. Phys.

10 Discuss., 15, 20597-20628, 10.5194/acpd-15-20597-2015, 2015a.

11 Fuhlbrügge, S., Quack, B., Tegtmeier, S., Atlas, E., Hepach, H., Shi, Q., Raimund, S., and

12 Krüger, K.: The contribution of oceanic halocarbons to marine and free troposphere air over

13 the tropical west Pacific, Atmos. Chem. Phys. Discuss., 15, 17887-17943, 10.5194/acpd-15-

14 17887-2015, 2015b.

15 Fuse, H., Inoue, H., Murakami, K., Takimura, O., and Yamaoka, Y.: Production of free and

16 organic iodine by roseovarius spp, FEMS Microbiology Letters, 229, 189-194,

17 10.1016/s0378-1097(03)00839-5, 2003.

18 Gómez Martín, J. C. G., Mahajan, A. S., Hay, T. D., Prados-Roman, C., Ordonez, C.,

19 MacDonald, S. M., Plane, J. M. C., Sorribas, M., Gil, M., Mora, J. F. P., Reyes, M. V. A.,

20 Oram, D. E., Leedham, E., and Saiz-Lopez, A.: Iodine chemistry in the eastern Pacific marine

21 boundary layer, J. Geophys. Res.-Atmos., 118, 887-904, 10.1002/jgrd.50132, 2013.

22 Grossmann, K., Friess, U., Peters, E., Wittrock, F., Lampel, J., Yilmaz, S., Tschritter, J.,

23 Sommariva, R., von Glasow, R., Quack, B., Kruger, K., Pfeilsticker, K., and Platt, U.: Iodine

24 monoxide in the western Pacific marine boundary layer, Atmos. Chem. Phys., 13, 3363-3378,

25 10.5194/acp-13-3363-2013, 2013.

26 Gschwend, P. M., Macfarlane, J. K., and Newman, K. A.: Volatile halogenated organic

27 compounds released to seawater from temperate marine macroalgae, Science, 227, 1033-

28 1035, 10.1126/science.227.4690.1033, 1985.

29 Hepach, H., Quack, B., Ziska, F., Fuhlbrügge, S., Atlas, E. L., Krüger, K., Peeken, I., and

30 Wallace, D. W. R.: Drivers of diel and regional variations of halocarbon emissions from the

Atmospheric
Chemistry
and Physics
Discussions

1   tropical north east Atlantic, Atmos. Chem. Phys., 14, 1255-1275, 10.5194/acp-14-1255-2014,

2   2014.

3   Hepach, H., Quack, B., Raimund, S., Fischer, T., Atlas, E. L., and Bracher, A.: Halocarbon

4   emissions and sources in the equatorial Atlantic cold tongue, Biogeosciences, 12, 6369-6387,

5   10.5194/bg-12-6369-2015, 2015.

6   Hill, V. L., and Manley, S. L.: Release of reactive bromine and iodine from diatoms and its

7   possible role in halogen transfer in polar and tropical oceans, Limnol. Oceanogr., 54, 812-

8   822, 10.4319/lo.2009.54.3.0812, 2009.

9   Hossaini, R., Chipperfield, M. P., Montzka, S. A., Rap, A., Dhomse, S., and Feng, W.:

10   Efficiency of short-lived halogens at influencing climate through depletion of stratospheric

11   ozone, Nat. Geosci., 8, 186-190, 10.1038/ngeo2363, 2015.

12   Hughes, C., Franklin, D. J., and Malin, G.: Iodomethane production by two important marine

13   cyanobacteria: prochlorococcus marinus (ccmp 2389) and synechococcus sp (ccmp 2370),

14   Mar. Chem., 125, 19-25, 10.1016/j.marchem.2011.01.007, 2011.

15   Hughes, C., Johnson, M., Utting, R., Turner, S., Malin, G., Clarke, A., and Liss, P. S.:

16   Microbial control of bromocarbon concentrations in coastal waters of the western Antarctic

17   peninsula, Mar. Chem., 151, 35-46, 10.1016/j.marchem.2013.01.007, 2013.

18   Jones, C. E., and Carpenter, L. J.: Solar photolysis of CH_2I_2, CH_2ICl, and CH_2IBr in water,

19   saltwater, and seawater, Environ. Sci. Technol., 39, 6130-6137, 10.1021/es050563g, 2005.

20   Jones, C. E., and Carpenter, L. J.: Chemical destruction of CH_3I, C_2H_5I, $1-C_3H_7I$, and $2-C_3H_7I$

21   in saltwater, Geophys. Res. Lett., 34, 10.1029/2007gl029775, 2007.

22   Jones, C. E., Hornsby, K. E., Sommariva, R., Dunk, R. M., Von Glasow, R., McFiggans, G.,

23   and Carpenter, L. J.: Quantifying the contribution of marine organic gases to atmospheric

24   iodine, Geophys. Res. Lett., 37, L1880410.1029/2010gl043990, 2010.

25   Karstensen, J., Stramma, L., and Visbeck, M.: Oxygen minimum zones in the eastern tropical

26   Atlantic and Pacific oceans, Prog. Oceanogr., 77, 331-350, 10.1016/j.pocean.2007.05.009,

27   2008.

28   Krüger, K., and Quack, B.: Introduction to special issue: the TransBrom Sonne expedition in

29   the tropical west Pacific, Atmos. Chem. Phys., 13, 9439-9446, 10.5194/acp-13-9439-2013,

30   2013.

Atmospheric
Chemistry
and Physics
Discussions

1   Lampel, J., Frieß, U., and Platt, U.: The impact of vibrational raman scattering of air on doas
2   measurements of atmospheric trace gases, Atmos. Meas. Tech., 8, 3767-3787, 10.5194/amt-8-
3   3767-2015, 2015.

4   Lawler, M. J., Mahajan, A. S., Saiz-Lopez, A., and Saltzman, E. S.: Observations of I_2 at a
5   remote marine site, Atmos. Chem. Phys., 14, 2669-2678, 10.5194/acp-14-2669-2014, 2014.

6   Lin, C. Y., and Manley, S. L.: Bromoform production from seawater treated with
7   bromoperoxidase, Limnol. Oceanogr., 57, 1857-1866, 10.4319/1o.2012.57.06.1857, 2012.

8   Liu, Y. N., Yvon-Lewis, S. A., Thornton, D. C. O., Campbell, L., and Bianchi, T. S.: Spatial
9   distribution of brominated very short-lived substances in the eastern Pacific, J. Geophys. Res.-
10 Oceans, 118, 2318-2328, 10.1002/jgrc.20183, 2013.

11 Liu, Y. N., Thornton, D. C. O., Bianchi, T. S., Arnold, W. A., Shields, M. R., Chen, J., and
12 Yvon-Lewis, S. A.: Dissolved organic matter composition drives the marine production of
13 brominated very short-lived substances, Environ. Sci. Technol., 49, 3366-3374,
14 10.1021/es505464k, 2015.

15 Mahajan, A. S., Plane, J. M. C., Oetjen, H., Mendes, L., Saunders, R. W., Saiz-Lopez, A.,
16 Jones, C. E., Carpenter, L. J., and McFiggans, G. B.: Measurement and modelling of
17 tropospheric reactive halogen species over the tropical Atlantic ocean, Atmos. Chem. Phys.,
18 10, 4611-4624, 10.5194/acp-10-4611-2010, 2010.

19 Mahajan, A. S., Gómez Martín, J. C., Hay, T. D., Royer, S. J., Yvon-Lewis, S., Liu, Y., Hu,
20 L., Prados-Roman, C., Ordóñez, C., Plane, J. M. C., and Saiz-Lopez, A.: Latitudinal
21 distribution of reactive iodine in the eastern Pacific and its link to open ocean sources, Atmos.
22 Chem. Phys., 12, 11609-11617, 10.5194/acp-12-11609-2012, 2012.

23 Manley, S. L., and de la Cuesta, J. L.: Methyl iodide production from marine phytoplankton
24 cultures, Limnol. Oceanogr., 42, 142-147, 10.4319/lo.1997.42.1.0142, 1997.

25 Martino, M., Liss, P. S., and Plane, J. M. C.: Wavelength-dependence of the photolysis of
26 diiodomethane in seawater, Geophys. Res. Lett., 33, 10.1029/2005gl025424, 2006.

27 Martino, M., Mills, G. P., Woeltjen, J., and Liss, P. S.: A new source of volatile organoiodine
28 compounds in surface seawater, Geophys. Res. Lett., 36, 10.1029/2008gl036334, 2009.

29 Moore, R. M., and Zafiriou, O. C.: Photochemical production of methyl-iodide in seawater, J.
30 Geophys. Res.-Atmos., 99, 16415-16420, 10.1029/94jd00786, 1994.

Atmospheric
Chemistry
and Physics
Discussions

Open Access

EGU

1   Moore, R. M., Geen, C. E., and Tait, V. K.: Determination of henry law constants for a suite

2   of naturally-occurring halogenated methanes in seawater, Chemosphere, 30, 1183-1191,

3   10.1016/0045-6535(95)00009-w, 1995.

4   Moore, R. M., Webb, M., Tokarczyk, R., and Wever, R.: Bromoperoxidase and

5   iodoperoxidase enzymes and production of halogenated methanes in marine diatom cultures,

6   J. Geophys. Res.-Oceans, 101, 20899-20908, 10.1029/96jc01248, 1996.

7   Moore, R. M., and Groszko, W.: Methyl iodide distribution in the ocean and fluxes to the

8   atmosphere, J. Geophys. Res.-Oceans, 104, 11163-11171, 10.1029/1998jc900073, 1999.

9   Nightingale, P. D., Malin, G., Law, C. S., Watson, A. J., Liss, P. S., Liddicoat, M. I., Boutin,

10 J., and Upstill-Goddard, R. C.: In situ evaluation of air-sea gas exchange parameterizations

11 using novel conservative and volatile tracers, Glob. Biogeochem. Cycles, 14, 373-387,

12 10.1029/1999gb900091, 2000.

13 O'Dowd, C. D., Jimenez, J. L., Bahreini, R., Flagan, R. C., Seinfeld, J. H., Hameri, K., Pirjola,

14 L., Kulmala, M., Jennings, S. G., and Hoffmann, T.: Marine aerosol formation from biogenic

15 iodine emissions, Nature, 417, 632-636, 10.1038/nature00775, 2002.

16 Peters, C., Pechtl, S., Stutz, J., Hebestreit, K., Honninger, G., Heumann, K. G., Schwarz, A.,

17 Winterlik, J., and Platt, U.: Reactive and organic halogen species in three different European

18 coastal environments, Atmos. Chem. Phys., 5, 3357-3375, 2005.

19 Prados-Roman, C., Cuevas, C. A., Hay, T., Fernandez, R. P., Mahajan, A. S., Royer, S. J.,

20 Galí, M., Simó, R., Dachs, J., Großmann, K., Kinnison, D. E., Lamarque, J. F., and Saiz-

21 Lopez, A.: Iodine oxide in the global marine boundary layer, Atmos. Chem. Phys., 15, 583-

22 593, 10.5194/acp-15-583-2015, 2015.

23 Quack, B., and Wallace, D. W. R.: Air-sea flux of bromoform: controls, rates, and

24 implications, Glob. Biogeochem. Cycles, 17, 10.1029/2002gb001890, 2003.

25 Quack, B., Atlas, E., Petrick, G., Stroud, V., Schauffler, S., and Wallace, D. W. R.: Oceanic

26 bromoform sources for the tropical atmosphere, Geophys. Res. Lett., 31,

27 10.1029/2004gl020597, 2004.

28 Quack, B., Atlas, E., Petrick, G., and Wallace, D. W. R.: Bromoform and dibromomethane

29 above the Mauritanian upwelling: atmospheric distributions and oceanic emissions, J.

30 Geophys. Res.-Atmos., 112, 10.1029/2006jd007614, 2007a.

40

Atmospheric
Chemistry
and Physics
Discussions

1 Quack, B., Peeken, I., Petrick, G., and Nachtigall, K.: Oceanic distribution and sources of
2 bromoform and dibromomethane in the Mauritanian upwelling, J. Geophys. Res.-Oceans,
3 112, 10.1029/2006jc003803, 2007b.

4 Raimund, S., Quack, B., Bozec, Y., Vernet, M., Rossi, V., Garcon, V., Morel, Y., and Morin,
5 P.: Sources of short-lived bromocarbons in the Iberian upwelling system, Biogeosciences, 8,
6 1551-1564, 10.5194/bg-8-1551-2011, 2011.

7 Read, K. A., Mahajan, A. S., Carpenter, L. J., Evans, M. J., Faria, B. V. E., Heard, D. E.,
8 Hopkins, J. R., Lee, J. D., Moller, S. J., Lewis, A. C., Mendes, L., McQuaid, J. B., Oetjen, H.,
9 Saiz-Lopez, A., Pilling, M. J., and Plane, J. M. C.: Extensive halogen-mediated ozone
10 destruction over the tropical Atlantic ocean, Nature, 453, 1232-1235, 10.1038/nature07035,
11 2008.

12 Richter, U., and Wallace, D. W. R.: Production of methyl iodide in the tropical Atlantic
13 ocean, Geophys. Res. Lett., 31, 10.1029/2004gl020779, 2004.

14 Saiz-Lopez, A., Lamarque, J. F., Kinnison, D. E., Tilmes, S., Ordonez, C., Orlando, J. J.,
15 Conley, A. J., Plane, J. M. C., Mahajan, A. S., Santos, G. S., Atlas, E. L., Blake, D. R.,
16 Sander, S. P., Schauffler, S., Thompson, A. M., and Brasseur, G.: Estimating the climate
17 significance of halogen-driven ozone loss in the tropical marine troposphere, Atmos. Chem.
18 Phys., 12, 3939-3949, 10.5194/acp-12-3939-2012, 2012a.

19 Saiz-Lopez, A., Plane, J. M. C., Baker, A. R., Carpenter, L. J., von Glasow, R., Martin, J. C.
20 G., McFiggans, G., and Saunders, R. W.: Atmospheric chemistry of iodine, Chem. Rev., 112,
21 1773-1804, 10.1021/cr200029u, 2012b.

22 Saiz-Lopez, A., Fernandez, R. P., Ordóñez, C., Kinnison, D. E., Gómez Martín, J. C.,
23 Lamarque, J. F., and Tilmes, S.: Iodine chemistry in the troposphere and its effect on ozone,
24 Atmos. Chem. Phys., 14, 13119-13143, 10.5194/acp-14-13119-2014, 2014.

25 Saiz-Lopez, A., Baidar, S., Cuevas, C. A., Koenig, T. K., Fernandez, R. P., Dix, B., Kinnison,
26 D. E., Lamarque, J. F., and Rodriguez-LLoveras, T. L.: Injection of iodine to the stratosphere,
27 Geophys. Res. Lett., 42, 6852-6859, 10.1002/2015GL064796, 2015.

28 Salawitch, R. J.: Atmospheric chemistry - biogenic bromine, Nature, 439, 275-277,
29 10.1038/439275a, 2006.

Atmospheric
Chemistry
and Physics
Discussions

1 Scarratt, M. G., and Moore, R. M.: Production of methyl bromide and methyl chloride in
2 laboratory cultures of marine phytoplankton II, Mar. Chem., 59, 311-320, 10.1016/s0304-
3 4203(97)00092-3, 1998.

4 Schauffler, S. M., Atlas, E. L., Flocke, F., Lueb, R. A., Stroud, V., and Travnicek, W.:
5 Measurements of bromine containing organic compounds at the tropical tropopause, Geophys.
6 Res. Lett., 25, 317-320, 10.1029/98GL00040, 1998.

7 Schönhardt, A., Richter, A., Wittrock, F., Kirk, H., Oetjen, H., Roscoe, H. K., and Burrows, J.
8 P.: Observations of iodine monoxide columns from satellite, Atmos. Chem. Phys., 8, 637-653,
9 10.5194/acp-8-637-2008, 2008.

10 Shi, Q., Marandino, C., Petrick, G., Quack, B., and Wallace, D.: A time series of incubation
11 experiments to examine the production and loss of CH_3I in surface seawater, J. Geophys.
12 Res.-Oceans, 119, 8242-8254, 10.1002/2014jc010223, 2014.

13 Smythe-Wright, D., Boswell, S. M., Breithaupt, P., Davidson, R. D., Dimmer, C. H., and
14 Diaz, L. B. E.: Methyl iodide production in the ocean: implications for climate change, Glob.
15 Biogeochem. Cycles, 20, 10.1029/2005gb002642, 2006.

16 Sommariva, R., and von Glasow, R.: Multiphase halogen chemistry in the tropical Atlantic
17 ocean, Environ. Sci. Technol., 46, 10429-10437, 10.1021/es300209f, 2012.

18 Stemmler, I., Hense, I., Quack, B., and Maier-Reimer, E.: Methyl iodide production in the
19 open ocean, Biogeosciences, 11, 4459-4476, 10.5194/bg-11-4459-2014, 2014.

20 Stohl, A., and Trickl, T.: A textbook example of long-range transport: simultaneous
21 observation of ozone maxima of stratospheric and North American origin in the free
22 troposphere over Europe, J. Geophys. Res.-Atmos., 104, 30445-30462,
23 10.1029/1999jd900803, 1999.

24 Stohl, A., Forster, C., Frank, A., Seibert, P., and Wotawa, G.: Technical note: the lagrangian
25 particle dispersion model flexpart version 6.2, Atmos. Chem. Phys., 5, 2461-2474,
26 10.5194/acp-5-2461-2005, 2005.

27 Tanhua, T., Fogelqvist, E., and Basturk, O.: Reduction of volatile halocarbons in anoxic
28 seawater, results from a study in the Black Sea, Mar. Chem., 54, 159-170, 10.1016/0304-
29 4203(96)00005-9, 1996.

Atmospheric
Chemistry
and Physics
Discussions

1 Taylor, B. B., Torrecilla, E., Bernhardt, A., Taylor, M. H., Peeken, I., Rottgers, R., Piera, J.,

2 and Bracher, A.: Bio-optical provinces in the eastern Atlantic ocean and their biogeographical

3 relevance, Biogeosciences, 8, 3609-3629, 10.5194/bg-8-3609-2011, 2011.

4 Tegtmeier, S., Krüger, K., Quack, B., Atlas, E., Blake, D. R., Boenisch, H., Engel, A.,

5 Hepach, H., Hossaini, R., Navarro, M. A., Raimund, S., Sala, S., Shi, Q., and Ziska, F.: The

6 contribution of oceanic methyl iodide to stratospheric iodine, Atmos. Chem. Phys., 13, 11869-

7 11886, 10.5194/acp-13-11869-2013, 2013.

8 Theiler, R., Cook, J. C., and Hager, L. P.: Halohydrocarbon synthesis by bromoperoxidase,

9 Science, 202, 1094-1096, 10.1126/science.202.4372.1094, 1978.

10 Tokarczyk, R., and Moore, R. M.: Production of volatile organohalogens by phytoplankton

11 cultures, Geophys. Res. Lett., 21, 285-288, 10.1029/94GL00009, 1994.

12 Tomczak, M., and Godfrey, J. S.: Regional oceanography: an introduction, 2 ed., Daya

13 Publishing House, Delhi, 2005.

14 Uitz, J., Claustre, H., Morel, A., and Hooker, S. B.: Vertical distribution of phytoplankton

15 communities in open ocean: an assessment based on surface chlorophyll, J. Geophys. Res.-

16 Oceans, 111, 10.1029/2005jc003207, 2006.

17 Varner, R. K., Zhou, Y., Russo, R. S., Wingenter, O. W., Atlas, E., Stroud, C., Mao, H.,

18 Talbot, R., and Sive, B. C.: Controls on atmospheric chloroiodomethane (CH_2ClI) in marine

19 environments, J. Geophys. Res.-Atmos., 113, D10303

20 10.1029/2007jd008889, 2008.

21 Vidussi, F., Claustre, H., Manca, B. B., Luchetta, A., and Marty, J. C.: Phytoplankton pigment

22 distribution in relation to upper thermocline circulation in the eastern Mediterranean Sea

23 during winter, J. Geophys. Res.-Oceans, 106, 19939-19956, 10.1029/1999jc000308, 2001.

24 von Glasow, R., von Kuhlmann, R., Lawrence, M. G., Platt, U., and Crutzen, P. J.: Impact of

25 reactive bromine chemistry in the troposphere, Atmos. Chem. Phys., 4, 2481-2497,

26 10.5194/acp-4-2481-2004, 2004.

27 White, R. H.: Analysis of dimethyl sulfonium compounds in marine-algae, J. Mar. Res., 40,

28 529-536, 1982.

29 Wurl, O., Wurl, E., Miller, L., Johnson, K., and Vagle, S.: Formation and global distribution

30 of sea-surface microlayers, Biogeosciences, 8, 121-135, 10.5194/bg-8-121-2011, 2011.

Atmospheric
Chemistry
and Physics
Discussions

Open Access

EGU

1 Yamamoto, H., Yokouchi, Y., Otsuki, A., and Itoh, H.: Depth profiles of volatile halogenated

2 hydrocarbons in seawater in the Bay of Bengal, Chemosphere, 45, 371-377, 10.1016/s0045-

3 6535(00)00541-5, 2001.

4 Yilmaz, S.: Retrieval of atmospheric aerosol and trace gas vertical profiles using multi-axis

5 differential optical absorption spectroscopy, Institut für Umweltphysik, Universität

6 Heidelberg, Heidelberg, Heidelberg, 2012.

7 Yokouchi, Y., Saito, T., Ooki, A., and Mukai, H.: Diurnal and seasonal variations of

8 iodocarbons (CH_2ClI, CH_2I_2, CH_3I, and C_2H_5I) in the marine atmosphere, J. Geophys. Res.-

9 Atmos., 116, 10.1029/2010jd015252, 2011.

10 Yokouchi, Y., Ooki, A., Hashimoto, S., and Itoh, H.: A study on the production and emission

11 of marine-derived volatile halocarbons, in: Western pacific air-sea interactions study, edited

12 by: Uematsu, M., Yokouchi, Y., Watanabe, Y. W., Takeda, S., and Yamanaka, Y.,

13 TERRAPUB, Okusawa, 1-25, 2014.

14 Zafiriou, O. C.: Reaction of methyl halides with seawater and marine aerosols, J. Mar. Res.,

15 33, 75-81, 1975.

16 Ziska, F., Quack, B., Abrahamsson, K., Archer, S. D., Atlas, E., Bell, T., Butler, J. H.,

17 Carpenter, L. J., Jones, C. E., Harris, N. R. P., Hepach, H., Heumann, K. G., Hughes, C.,

18 Kuss, J., Krüger, K., Liss, P., Moore, R. M., Orlikowska, A., Raimund, S., Reeves, C. E.,

19 Reifenhäuser, W., Robinson, A. D., Schall, C., Tanhua, T., Tegtmeier, S., Turner, S., Wang,

20 L., Wallace, D., Williams, J., Yamamoto, H., Yvon-Lewis, S., and Yokouchi, Y.: Global sea-

21 to-air flux climatology for bromoform, dibromomethane and methyl iodide, Atmos. Chem.

22 Phys., 13, 8915-8934, 10.5194/acp-13-8915-2013, 2013.